



Energy Local Storage Advanced system

D6.4 Technical impact analysis and proof-of-concept on system level

November 2018

Imprint

Technical impact analysis and proof-of-concept on system level, November 2018

Contractual Date of Delivery to the EC:	30.11.2018
Actual Date of Delivery to the EC:	30.11.2018
Author(s):	Michael Diekerhof, Diala Nouti, Manuel Pitz, Nikolaus Wirtz (All authors are with the Institute for Automation of Complex Power Systems at RWTH Aachen University)
Participant(s):	BYES, REN, RWTH, AUEW
Project:	Energy Local Storage Advanced system (ELSA)
Work package:	WP6 - Design optimization and technical impact analysis
Task:	6.4 - Technical impact analysis on system level
Estimated person months:	17
Confidentiality:	Public
Version:	V1.0
Contact:	Michael Diekerhof <mdiekerhof@eonerc.rwth-aachen.de>
Website:	www.elsa-h2020.eu

Legal disclaimer

The project Energy Local Storage Advanced system (ELSA) has received funding from the European Union's Horizon 2020 research and innovation programme under grant agreement No 646125. The sole responsibility for the content of this publication lies with the authors. It does not necessarily reflect the opinion of the Innovation and Networks Executive Agency (INEA) or the European Commission (EC). INEA or the EC are not responsible for any use that may be made of the information contained therein.

Copyright

© The ELSA consortium – Energy Local Storage Advanced system, contact@ELSA-h2020.eu, <http://www.ELSA-h2020.eu/Contact.html>. Copies of this publication – also of extracts thereof – may only be made with reference to the publisher.

Executive Summary

The Energy Local Storage Advanced system (ELSA) project aims at the deployment of affordable battery energy storage system solutions including battery management and optimization software. Energy storage is considered a key technology within the energy supply system, in which an increasing number of distributed generators make use of volatile Renewable Energy Sources (RESs) with a fluctuating power output behaviour.

In comparison to conventional energy storage systems such as pumped-storage power plants, battery storage systems are primarily used to compensate power fluctuations on a local level but can additionally provide individual services to different stakeholders, e.g., to the end-customers or Distributions System Operators (DSOs).

ELSA addresses this urgent need for local energy solutions and provides required services by introducing the ELSA battery storage system as a combination of second-life lithium ion batteries and required power electronic devices. It directly interfaces towards the low-voltage power grid, as its main purpose is to support the local grid by providing its flexibility potential to the power supply system. This leads to both grid stabilizing and economically meaningful use cases such as peak shaving, participation to energy trade market, primary control reserve, energy cost minimization and others.

The advantage of the ELSA system in comparison to existing battery storage systems is in the usage of second-life lithium ion batteries, which were formerly used in electric vehicles in their first life. A focus is set on minimal reassembling costs, therefore, the entire battery pack is taken from a vehicle and directly connected to the inverter hardware developed in this project. The recycling and gentle use of resources is in general an important aspect of economy and the reuse of such electric vehicle batteries results in a massive extension in lifetime. This lifetime extension results in a decreased carbon footprint over lifetime and reduces the waste production as well as the mining of rare resources to build new battery cells. Leveraging the modularity of the battery storage system, ELSA further enables scalable solutions for the abovementioned use case scenarios. On these grounds, the benefits and limitations for such a scalable approach are investigated in this deliverable.

The present work is intended to primarily quantify the technical impact of the scalable ELSA system. It addresses specific use case analyses that are enabled by large-scale ELSA storage applications such as primary control reserve. It is shown that depending on the use case considered, up to 20 ELSA storage systems are required to achieve feasible solutions leading to a significant techno-economic impact. Even larger systems are identified to be of interest in order to increase the cost efficiency.

Further, to understand the technical interactions between the individual ELSA storage systems as coordinated by a central controller unit, the behaviour of the communication between this

controller unit and the ELSA battery storage system is evaluated in this deliverable. For this purpose, an appropriate hardware in the loop setup is implemented, which serves as the basis for different communication tests performed. The setup contains a real controller unit and a simulation system, which is capable to simulate up to 1 000 ELSA storage systems. Different communication tests revealed that 50 ELSA storage systems can be aggregated with low latency under a parallel communication setup in comparison to a sequential one. However, the aggregation of more than 50 ELSA storage systems is still possible but comes with the costs of an increased latency. Based on this outcome, it is demonstrated that a sufficient number of ELSA storage systems can be aggregated to one big battery storage system in order to apply the investigated large-scale use cases in real life applications, which finally proves the maturity level and the technical concept of the ELSA system design.

Table of Contents

COPYRIGHT.....	2
EXECUTIVE SUMMARY	3
TABLE OF CONTENTS.....	5
LIST OF FIGURES.....	8
LIST OF TABLES	11
LIST OF ACRONYMS AND ABBREVIATIONS.....	12
1 INTRODUCTION.....	14
2 DT5 SYSTEM AND SECOND-LIFE BATTERIES.....	15
2.1 DT5 System.....	15
2.2 Second-life Batteries and ELSA BESS.....	16
2.3 Modelling	17
2.3.1 BESS Model for the Large-scale Use Case Simulations	17
2.3.2 BESS Model for the HiL Simulation	18
3 IMPACT ANALYSIS ON SPECIFIC USE CASES FOR LARGE-SCALE APPLICATIONS	23
3.1 Introduction.....	23
3.2 Metrics	23
3.2.1 Electrical Energy Costs	23
3.2.2 Imbalances and Imbalance Costs.....	23
3.2.3 Balancing Power Market Profit.....	24
3.3 Impact Analysis for National Energy Trade Market Participation.....	24
3.3.1 Use Case Description	25
3.3.2 Results.....	29
3.3.3 Conclusion.....	32
3.4 Impact Analysis for Balancing Group Optimization	32
3.4.1 Use Case Description	33

3.4.2	Results.....	35
3.4.3	Conclusion.....	37
3.5	Impact Analysis for Primary Reserve Control Participation.....	38
3.5.1	Use Case Description	40
3.5.2	Results.....	43
3.5.3	Conclusion.....	45
3.6	Use cases comparison	45
4	HIL SIMULATION	48
4.1	Introduction.....	48
4.2	Overall Hil Setup	49
4.2.1	Communication Simulation	49
4.2.2	IEC61850 Server.....	50
4.2.3	VILLASWeb User Interface	51
4.2.4	Controller DUT.....	52
4.2.5	CC to RTS Communication and Trigger	55
4.3	Test Conditions for Case Studies.....	55
4.3.1	Case Study 1.....	55
4.3.2	Case Study 2.....	56
4.4	System Characterization.....	57
4.4.1	Hardware and Setup Description.....	58
4.4.2	Connection Characterization RTS and SC.....	59
4.4.3	Connection Characterization Analogue CC to RTS Connection.....	62
4.4.4	Connection Characterization CC and RTS in Sequential Approach	62
4.4.5	Connection Characterization between CC, Switch and SC in Sequential Approach	64
4.4.6	Connection Characterization CC and SC in Parallel Approach	64
4.4.7	Performance Evaluation of the Power Allocation Algorithm.....	67
4.5	Results.....	68
4.5.1	Results Case Study 1	68
4.5.2	Results Case Study 2	69
4.6	Conclusion	70
5	CONCLUSIONS AND LESSONS LEARNED	71
	REFERENCES	73

ANNEX A: MATHEMATICAL OPTIMIZATION MODEL FOR THE LARGE-SCALE BESS USE CASE SIMULATIONS	77
ANNEX B: PARTICIPATION TO THE NATIONAL ENERGY TRADE MARKET USE CASE – MATHEMATICAL OPTIMIZATION PROBLEM FORMULATION	80

List of Figures

Figure 1: ELSA DT5 system power electronics and controllers installed at the RWTH Aachen pilot	15
Figure 2: ELSA second-life lithium ion battery packs installed at the RWTH Aachen pilot	16
Figure 3: System model setup including the large-scale BESS, Source: Adapted from [3]	17
Figure 4: Simple aggregated BESS model for the HiL simulation comprising two BESSs.....	18
Figure 5: Simulated model implemented in RSCAD	19
Figure 6: Battery model equivalent electrical circuit, Source: [6]	20
Figure 7: 3L-NPC inverter model implemented in RSCAD.....	21
Figure 8: Inverter PQ control scheme	22
Figure 9: Neutral-point voltage balancing control structure	22
Figure 10: System design for the participation to the national energy trade market use case	26
Figure 11: First stage of the MPC rolling optimization	28
Figure 12: City district power demand and local PV power generation during the considered summer week	29
Figure 13: Traded power for product A during the considered summer week.....	30
Figure 14: Traded power for product B during the considered summer week	30
Figure 15: Traded power for product C during the considered summer week	30
Figure 16: Battery storage operation depending on the balancing group situation	33
Figure 17: Balancing group management – cost objective	36
Figure 18: Balancing group management – imbalance objective.....	37
Figure 19: Principle of control reserve utilization in the German market, Source: [23]	38
Figure 20: Primary control reserve - optional overfulfillment, Source: Adapted from [24].....	41
Figure 21: Primary control reserve – dead-band usage, Source: Adapted from [24].....	41

Figure 22: Primary control reserve – market transactions, Source: Adapted from [24]	41
Figure 23: BESS SoC for the three different reserve control scenarios	43
Figure 24: BESS power provided to the grid for scenario 1	44
Figure 25: BESS power provided to the grid for scenario 2	44
Figure 26: BESS power provided to the grid for scenario 3	44
Figure 27: Primary control reserve price trend.....	45
Figure 28: Price development for lithium ion battery systems and power electronics, Source: Adapted from [26]	46
Figure 29: Investment cost and profit value for different use cases	47
Figure 30: HiL schema	49
Figure 31: HiL system setup	49
Figure 32: VILLASweb user interface.....	52
Figure 33: Architecture of a large-scale BESS	52
Figure 34: Flowchart of the power allocation algorithm for the active power control, Source: [31].....	53
Figure 35: Case study 1 – Sequential approach with active connections (first, access to BESS (2); then access to BESS (3))	56
Figure 36: Case study 2 – Semi-parallel BESS access (active connection to BESS (2) and idle connection to the other BESS)	57
Figure 37: Dell PowerEdge R440 SC installed at the RWTH Aachen pilot.....	58
Figure 38: WAGO 750-8206 PFC200 installed at the RWTH Aachen pilot.....	58
Figure 39: General test setup without switch.....	59
Figure 40: General test setup with switch	59
Figure 41: Fast update rate RTS to SC communication.....	60
Figure 42: Slow update rate RTS to SC communication.....	61
Figure 43: WAGO 750-559 analogue rise time (left) and fall time (right).....	62
Figure 44: Communication latency between RTS and CC with sequential approach.....	63
Figure 45: Communication latency CC to RTS including switch, with sequential approach.....	64

Figure 46: Communication latency CC to RTS including switch with parallel approach.....	65
Figure 47: Increase in mean delay over the number of BESS with parallel approach	66
Figure 48: Communication latency CC to RTS including switch with parallel approach (fixed and free run)	67
Figure 49: Communication latency full system with sequential approach.....	68
Figure 50: Communication latency full system with parallel approach.....	69

List of Tables

Table 1: Evaluation and comparison of the metric values for different energy commodities and the district operator’s total energy costs during the considered summer week for a scenario with ELSA BESS and a scenario without ELSA BESS.....	31
Table 2: Battery operation strategies for balancing group management	34
Table 3: BESS parameters for the ELSA DT5 system in the primary control reserve context.....	40
Table 4: Comparison of the potential for the different large-scale use cases with upscaled BESS.....	46
Table 5: Configuration for characterization of connection between RTS and SC.....	60
Table 6: Statistics characterization RTS to SC communication	61
Table 7: Test configurations for the sequential write test.....	63
Table 8: Statistics characterization CC to RTS communication with sequential approach.....	63
Table 9: Statistics characterization CC to RTS communication including switch with sequential approach.....	64
Table 10: Statistics characterization CC to RTS communication including switch with parallel approach	66
Table 11: Statistics characterization CC to RTS communication including switch with parallel approach (fixed and free run)	67
Table 12: Power allocation algorithm measured runtime	68
Table 13: Statistics CC to RTS including switch latency with sequential approach	69
Table 14: Statistics of full system test with parallel approach.....	70

List of Acronyms and Abbreviations

3L-NPC	Three-Level Neutral-Point Clamped
BESS	Battery Energy Storage System
CC	Coordinated Controller
DSO	Distribution System Operator
DUT	Device Under Test
EEG	“Erneuerbare-Energien-Gesetz”
ELSA	Energy Local Storage Advanced system
HiL	Hardware in the Loop
ICD	IED Capability Description
ICT	Information and Communication Technology
IED	Intelligent Electronic Device
MMS	Manufacturing Message Specification
MPC	Model Predictive Control
PCC	Point of Common Coupling
PCS	Power Converter System
PLC	Programmable Logic Controller
PWM	Pulse Width Modulation
RES	Renewable Energy Source
RTDS	Real-Time Digital Simulator
RTS	Real-Time Simulator
SC	Simulation Computer
SoC	State of Charge
SoD	State of Discharge
SRF	Synchronous Reference Frame
SV	Sampled Values
SVM	Space Vector Modulation
TSO	Transmission System Operator
VPP	Virtual Power Plant
WP	Work Package

1 Introduction

The Energy Local Storage Advanced system (ELSA) project aims at the deployment of affordable battery energy storage system solutions including battery management and optimization software. Energy management systems based on Information and Communication Technology (ICT) on local (building), community district and system scale level are designed and integrated in each project demonstration site to optimally manage and control the flexible devices including the ELSA battery energy storage. In this context, Work Package (WP) 6 aims at supporting the design and validation of the ELSA's energy management solution by a dedicated environment. Furthermore, WP6 shall perform the technical impact analysis on system level as well as the evaluation of the quality of the offered services.

ELSA WP6 consists of four tasks. The first task, i.e., Task 6.1, focused on developing the required component and system level models to support the tests of the interaction of the developed energy management with second-life batteries and local energy resources as well as with the electrical grid. Tasks 6.2 and 6.3 focused on data acquisition and technical impact assessment of the services provided in the individual trials. Potential technical constraints were identified and conclusions and recommendations were drawn based on the experience that was obtained at the different ELSA pilots as presented in the ELSA Deliverable 6.3 [1]. Although the ELSA project is clearly a demonstration project comprising multifarious field tests, larger scenarios are evaluated in simulations because field tests are always limited in size and feasibility. However, large-scale simulation scenarios reveal different challenges compared to field tests. For this purpose, Task 6.4 is intended to analyse such upscaled scenarios. The scenarios for the upscaled simulations are defined in this deliverable and implemented in appropriate simulation tools. Modelling of components is performed representing the level of detail that is required for these analyses. In addition, a proof of concept evaluation will be possible on system level.

Together with Deliverable 6.3, Deliverable 6.4 is the final deliverable of WP6 and provides the impact analysis for upscaled scenarios covering different ELSA use cases for large-scale Battery Energy Storage System (BESS) applications as well as the technical analysis of the BESS communication infrastructure. A sophisticated communication infrastructure design is the requirement for the control of multiple BESSs aggregated to one system. This aggregated BESS is the prerequisite for certain use cases which require larger BESS power and capacity installations to fulfil regulatory requirements or to be economically viable. The models used in that context are presented in chapter 2 and serve as the basis for the large-scale use case evaluations in chapter 3 as well as the evaluation of the communication infrastructure in chapter 4. Finally, chapter 5 draws conclusions on the impact analysis resulting from the simulation scenarios and provides technical recommendations for the implementation of large-scale BESSs.

2 DT5 System and Second-life Batteries

The investigation of an upscaled BESS in Deliverable 6.4 is based on the latest ELSA BESS. More precisely, it is investigated in the latest ELSA DT5 system which is deployed at the pilots in La Défense in Paris, France and at the RWTH Aachen University in Aachen, Germany.

2.1 DT5 System

The DT5 system provides an update of the power electronics and controllers, see Figure 1, enabling the ELSA BESS a faster reaction to external control commands compared to DT3 and DT4 as well as a higher charging power. While the first versions of the ELSA BESS offered a maximum charging power of 3 kW and a maximum discharging power of 12 kW per battery pack, DT5 provides a symmetrical charging and discharging power of at most 12 kW.

In addition to the enhancement of the individual batteries of the ELSA BESS, DT5 aims to offer the ability of aggregating several BESS to a larger system by using a hierarchical communication and control architecture, with a coordinated controller responsible for distributing commands for the aggregated system to the individual BESSs. The communication and control architecture is explained in more detail in chapter 4.



Figure 1: ELSA DT5 system power electronics and controllers installed at the RWTH Aachen pilot

2.2 Second-life Batteries and ELSA BESS

ELSA aims at offering a storage-as-a-service system based on cost competitive second-life lithium ion battery energy storage and an interoperable ICT platform. With the recent acceleration of the electric vehicle market, the development of lithium ion battery technology has reached the maturity level. The need of very reliable and long lasting battery to answer the severe constraints of an automotive environment has led to the development of a mass production and affordable battery that can be also used for static storage applications.

At the ELSA pilots, second-life lithium ion batteries from Nissan Leaf and Renault Kangoo ZE vehicles are used. A second-life battery pack is composed of multiple cells connected to sensors, a controller, and other components and then housing the unit in a case, see Figure 2. The battery packs for both the Nissan Leaf and the Renault Kangoo ZE are composed of connecting 48 modules in a series. The packs for both the Nissan Leaf and the Renault Kangoo ZE are designed with a voltage of 360 V and provide a capacity of 11 kWh in the second-life application. One ELSA BESS may comprise up to eight of such packs leading to a total battery storage capacity of at most 88 kWh.

In the next section, the modelling of the ELSA BESS is presented taking into account the parameters and physical conditions as stated above.



Figure 2: ELSA second-life lithium ion battery packs installed at the RWTH Aachen pilot

2.3 Modelling

This deliverable requires the development of simulation models for large-scale second-life battery storage applications. In particular, the outcome of this deliverable aims to provide models and tools for enabling the large-scale analyses of different system level use cases. The focus is on the investigation of the impact of ELSA storage applications together with an efficient energy management system on a system level rather than on a single component level. In other words, this means that the focus is not on single ELSA BESS applications, but rather on the control and operation of multiple ELSA BESSs aggregated to one large system. The derived models are based on validated approaches and take into account already existing approaches in the literature.

2.3.1 BESS Model for the Large-scale Use Case Simulations

The large-scale use case simulations performed in chapter 3 rest on the mathematical optimization model as already defined and deployed in the confidential ELSA Deliverable 6.1 [2], compare Annex A, as well as on earlier work done in [3]. In this model, the operation of the intelligent coordination of an electrical large-scale BESS is formulated as a mathematical optimization model with the system setup as pictured in Figure 3. The motivation behind this mathematical model is to precisely map the physical relations shown in Figure 3 in order to perform several feasibility studies. The model comprises not only the BESS itself but also other local conditions depending on the considered use case, such as a connection to the main grid, the local PV power generation feed-in or the local city district power demand. For this purpose, the basic idea is to link the different power flows depicted in Figure 3 in a way that a power balance at the Common Point of Coupling (PCC) is always maintained. Additionally, the developed optimization model enables one to easily vary and analyse different use case objectives and/or component setups, since the model is configurable, reusable and extendable.

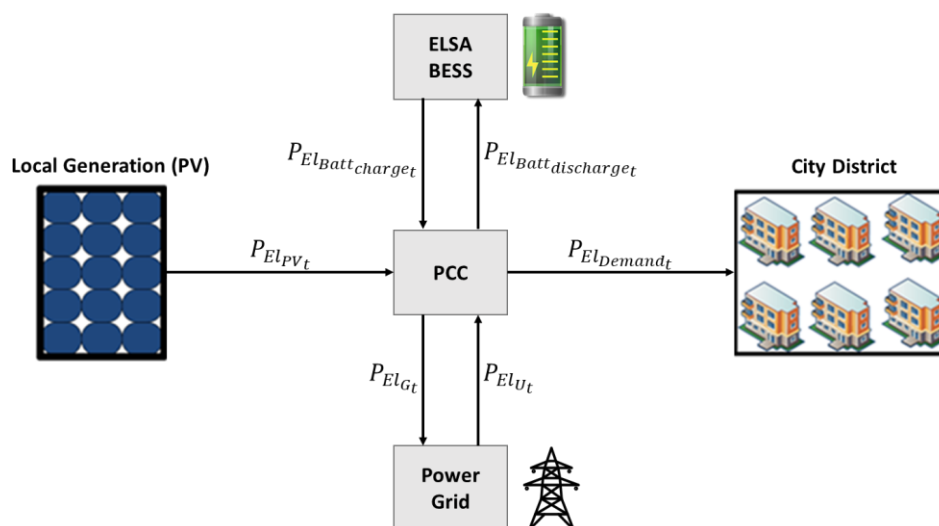


Figure 3: System model setup including the large-scale BESS, Source: Adapted from [3]

2.3.2 BESS Model for the HiL Simulation

In the Hardware in the Loop (HiL) setup, see section 4.2, a large-scale energy storage system is to be examined in a simulation environment. With the objectives of the validation of BESS aggregation and the examination of the communication performance limits of aggregation, a simplified model of an aggregated BESS and the grid is simulated. The simple model includes only two BESSs, where each BESS is interfaced to the grid through an AC/DC converter as shown in Figure 4. The model includes two BESSs only, since the focus of the HiL setup is on the communication performance and not on the validation of the electrical system. Nevertheless, the scaling up of the two BESSs is implemented in the communication simulation software in section 4.2.1 though.

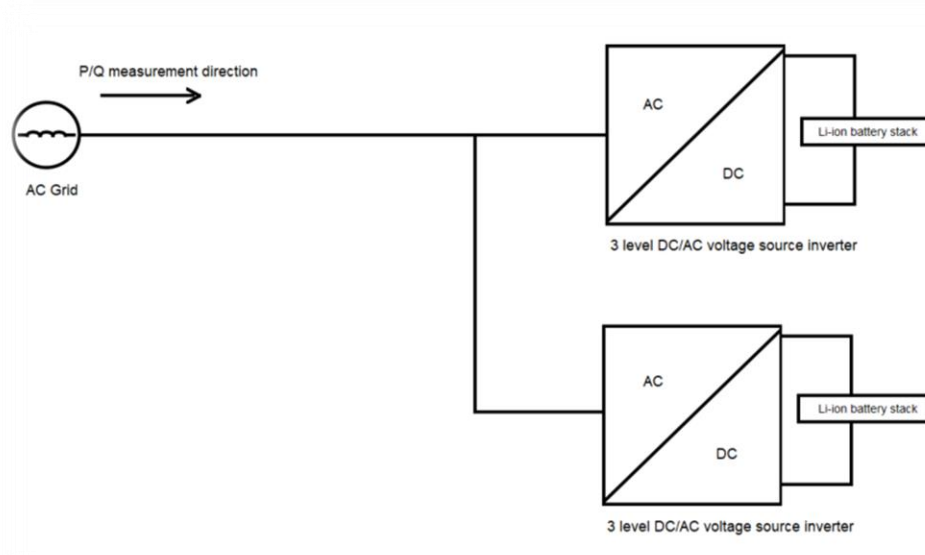


Figure 4: Simple aggregated BESS model for the HiL simulation comprising two BESSs

Before performing the real-time simulation of the electrical system, the model of the grid and the aggregated BESS was implemented in RSCAD [4], a commercial simulator software for power grid modelling which interfaces the Real Time Digital Simulator (RTDS) provided by RTDS Technologies Inc. [5]. The RSCAD model is depicted in Figure 5. For the sake of simplification, the system is simulated and evaluated under normal operation conditions only.

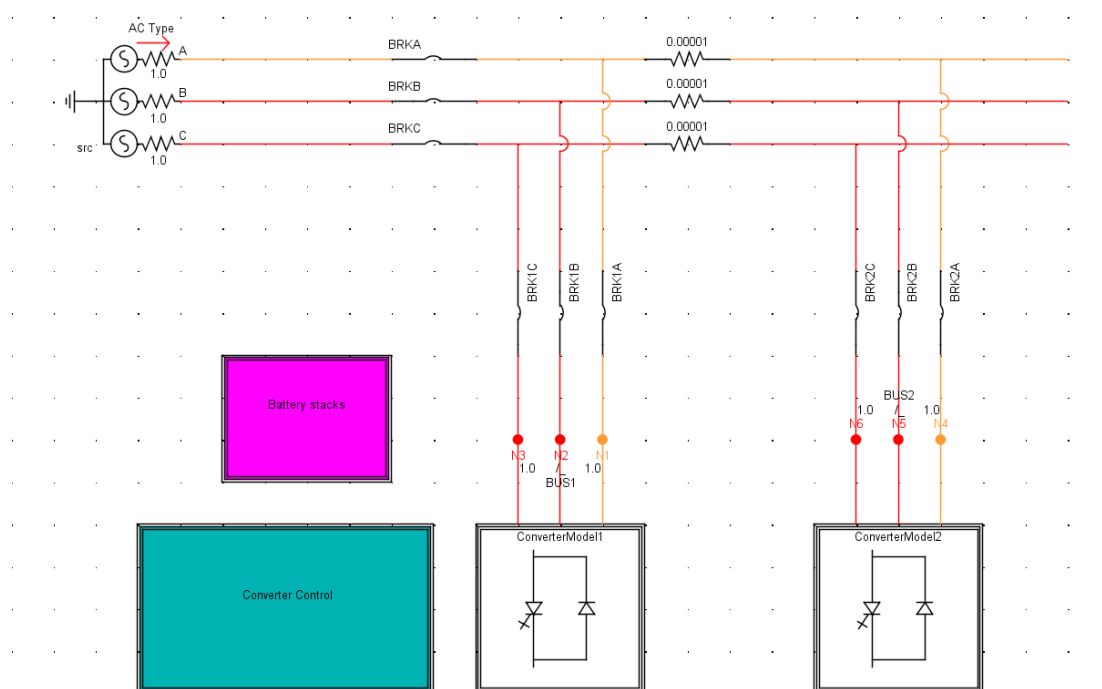


Figure 5: Simulated model implemented in RSCAD

As shown in Figure 5, the grid is modelled as a simple AC source that can both consume and inject infinite amounts of active and reactive power. As for the rest of the system, it is contained in the following three main blocks:

- Battery stacks
- Converter model
- Converter control

2.3.2.1 Battery Stacks

Because of the light weight, long life-span, and the maturity of this technology, lithium ion batteries are common for both electrical vehicles and energy storage devices. Hence, the battery stack model is based on the polymer lithium ion battery model proposed in [6]. The equivalent electrical circuit model, employing two time constants for short-term and long-term transients, is shown in Figure 6.

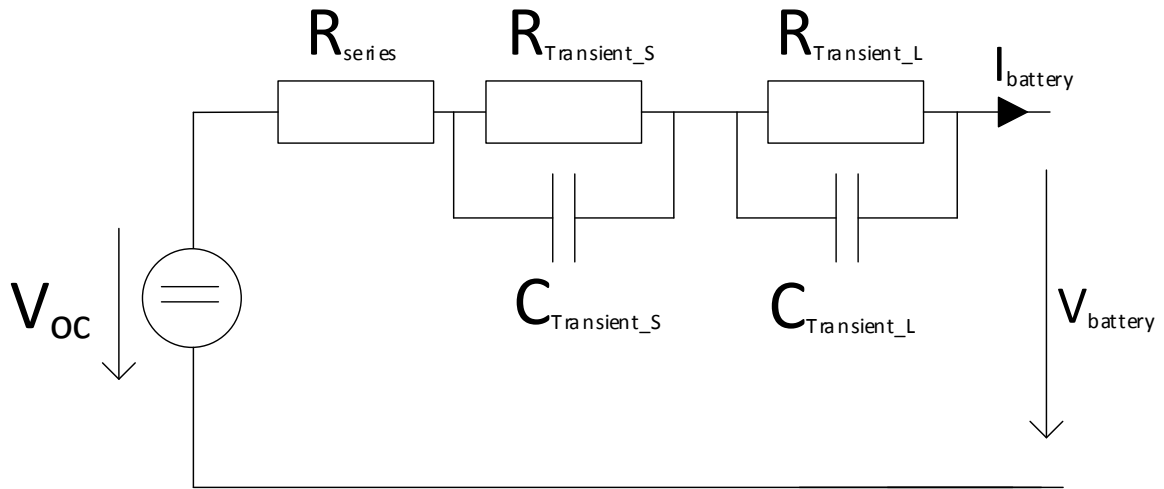


Figure 6: Battery model equivalent electrical circuit, Source: [6]

All the circuit parameters presented in Figure 6 are a function of the battery State of Charge (SoC), which is defined between 0% and 100% in this work. For the 850-mAh TCL PL-383562 polymer lithium ion batteries, the parameters are given as shown in equations (2.1) – (2.6) [6].

$$V_{OC}(\text{SoC}) = -1.031 e^{-35 \cdot \text{SoC}} + 3.685 + 0.2156 \cdot \text{SoC} - 0.1178 \cdot \text{SoC}^2 + 0.3201 \cdot \text{SoC}^3 \quad (2.1)$$

$$R_{\text{Series}}(\text{SoC}) = 0.1562 e^{-24.37 \cdot \text{SoC}} + 0.07446 \quad (2.2)$$

$$R_{\text{Transient}_S}(\text{SoC}) = 0.3208 e^{-29.14 \cdot \text{SoC}} + 0.04669 \quad (2.3)$$

$$C_{\text{Transient}_S}(\text{SoC}) = -752.9 e^{-13.51 \cdot \text{SoC}} + 703.6 \quad (2.4)$$

$$R_{\text{Transient}_L}(\text{SoC}) = 6.603 e^{-152.2 \cdot \text{SoC}} + 0.04984 \quad (2.5)$$

$$C_{\text{Transient}_L}(\text{SoC}) = -6056 e^{-27.12 \cdot \text{SoC}} + 4475 \quad (2.6)$$

As aforementioned, the focus of the HiL setup is in the evaluation of the communication performance limits of the ELSA large-scale system and not in the validation of the ELSA BESS electrical system. Hence, the TCL PL-383562 polymer lithium ion battery model (2.1) – (2.6) is used for the battery storage modelling in the HiL setup.

2.3.2.2 Converter Model

Each single BESS is connected to the grid through an AC/DC converter. The inverter model is based on a Three-Level Neutral-Point-Clamped (3L-NPC) inverter, which is connected to the grid through an L-filter, as shown in Figure 7. As the name indicates, the three-level inverter creates three different possible values for the phase-to-neutral output voltage, hence it results in $2 \cdot 3 + 1$ different voltage levels for the line-to-line voltage in a three-phase system. One of the main advantages of the 3L-NPC inverter is in the reduced harmonics in the output voltage. On the other hand, the neutral-point voltage unbalance is a typical problem of such 3L-NPC inverters [7]. To overcome this issue, converter control strategies are required as explained in the next subsection.

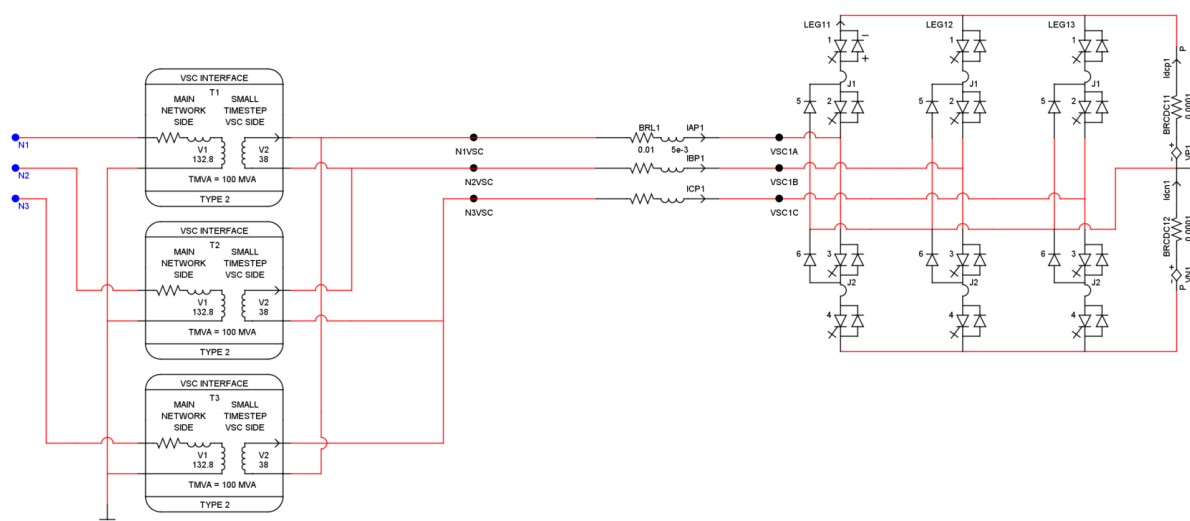


Figure 7: 3L-NPC inverter model implemented in RSCAD

2.3.2.3 Converter Control

The main goal of the converter control is to set the active power and reactive power set-points of the aggregated BESS. Hence, a decoupled PQ control strategy in the Synchronous Reference Frame (SRF) is implemented, using proportional integral controllers. The PQ references are used for generating a three-phase reference voltage. This voltage is divided by the DC-link voltage resulting in the Pulse Width Modulation (PWM) index as shown in Figure 8.

For the PWM scheme, sinusoidal PWM is used, where a sinusoidal modulation signal is compared with a high frequency triangle wave signal.

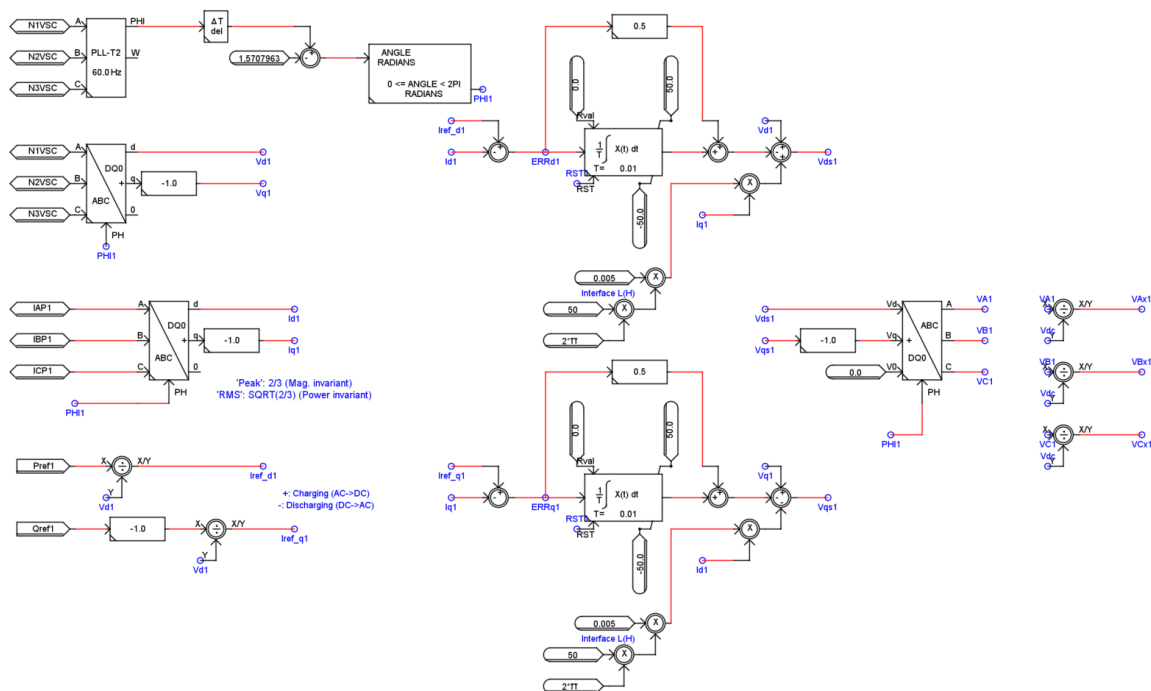


Figure 8: Inverter PQ control scheme

As aforementioned, the 3L-NPC inverter suffers from the neutral-point voltage balance problem. In the literature, various solutions are proposed, where some of these solutions are based on Space Vector Modulation (SVM) strategies [8, 9]. SVM makes use of the redundancy in many of the switching states which produce the same output voltage. Another approach is to use a multiple-carrier PWM to keep the neutral-point voltage balance [10]. However, the solution implemented here is based on the DC common mode voltage injection method, where a DC voltage offset is injected to the modulation reference voltages. This offset results in a current flow into the neutral point which restores the neutral point voltage balance [11]. This neutral point voltage balancing control structure is shown in Figure 9.

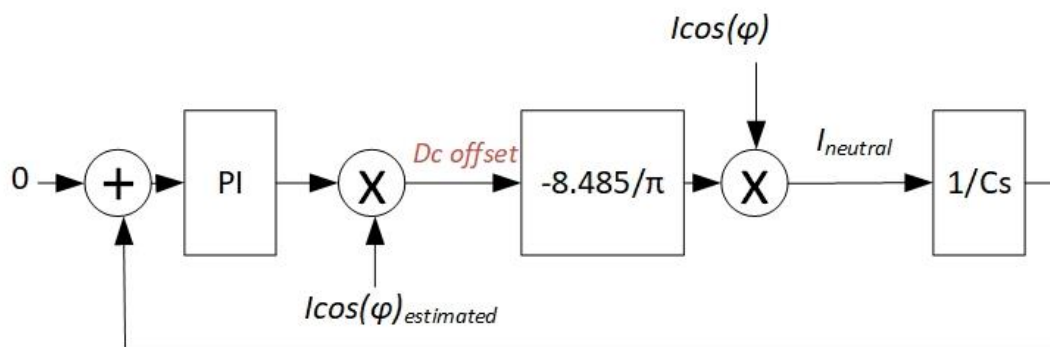


Figure 9: Neutral-point voltage balancing control structure

3 Impact Analysis on Specific Use Cases for Large-scale Applications

3.1 Introduction

This section describes the outcome of the simulations and optimizations for different use cases for the upscaled ELSA system. The metrics that are required to evaluate the performance of the outcome are explained as well as the methodology of each simulated use case. Note that the analyses for the use cases are based upon the specific optimization problem formulation introduced in section 2.3.1. As the analysed use cases are enabled by the utilization of an upscaled system, both the optimization algorithms and the results cannot be compared to the algorithms and results from the ELSA trial site implementations, which are limited in size and storage capacity. Thus, in order to quantify the benefit of specific use cases that cannot be deployed in real field trials, the developed optimization problem formulations are necessary for the large-scale service evaluations.

3.2 Metrics

For the assessment of the optimization results, appropriate metrics have already been defined in the confidential ELSA Deliverable 6.1 [2]. Some of these metrics, such as the energy imbalances and imbalance costs will be also used for the evaluation of the use cases for the upscaled ELSA system. However, as the up-scaling of the ELSA system enables additional use cases that are evaluated here, additional metrics have to be defined, specifically electrical energy costs and balancing power market profit.

3.2.1 Electrical Energy Costs

The total electrical energy costs in Euros are considered to evaluate the effect of, for instance, energy trading and do quantify the monetary effect (benefits/savings) of the specific use case. In a general form, the total electrical energy costs C_{tot} are calculated according to equation (3.1), where $E_{i,t}$ (in kWh) is a certain energy commodity i during time step t that is either purchased or sold under the specific costs $C_{i,t}$ (in $€/kWh$).

$$C_{tot} = \sum_i \sum_t E_{i,t} \cdot C_{i,t} \quad (3.1)$$

3.2.2 Imbalances and Imbalance Costs

For the Balancing Group Optimization use case, compare section 3.4, the total electrical energy imbalances $E_{imbalance,tot}$ in (3.2) are analysed where the imbalances before the optimization serve as a reference to the results after the optimization. These imbalances are also linked with the resulting imbalance costs C_{tot} in (3.3), calculated from the product of energy imbalances and the respective price, in order to quantify the savings of the optimization strategy.

$$E_{imbalance,tot} = \sum_t |E_{imbalance,t}| \quad (3.2)$$

$$C_{tot} = \sum_t E_{imbalance,t} \cdot C_t \quad (3.3)$$

3.2.3 Balancing Power Market Profit

For the Balancing Power Market use case, compare section 3.5, the profit for providing a certain power band for primary balancing power purposes is taken into account. This profit B is calculated according to equations (3.4) and (3.5) from the power band that is available over the course of one week and the respective price during that week.

$$B = P_{available,symmetrical} * Price_{PRC} \quad (3.4)$$

$$P_{available,symmetrical} = \min(|P_{available,negative}|, |P_{available,positive}|) \quad (3.5)$$

3.3 Impact Analysis for National Energy Trade Market Participation

The objective of this use case is in the participation to the national energy trade market to enable district operators to supply their districts with cheap energy as directly purchased from the energy trade market. This includes the usage of ELSA storage capabilities in order to buy or sell energy on the energy trade market to minimize the overall energy costs for district operators such as exemplarily demonstrated for the German pilot district in Kempten managed by Allgäuer Überlandwerke GmbH (AÜW) [12] in this use case analysis. Thus, the following use case results reflect German energy market conditions, but are quantitatively transferable to all other European countries which are subject to liberalized energy markets.

The national energy trade market participation use case is intended to choose the most economic market prices for energy trading along different energy spot market products available, e.g., day-ahead auction, intraday auction and intraday continuous. Moreover, this use case may also include – but is not limited to – the local generation of energy within a district, for instance as obtained from residential rooftop PV installations or local combined heat and power plants. In that case, it might be worth it to additionally use the ELSA BESS for local power balancing purposes, if and only if the storage usage would further decrease the district operator's energy costs to supply for its district.

3.3.1 Use Case Description

The participation to the national energy trade market use case is realized as a mixed-integer linear programming optimization problem embedded in a Model Predictive Control (MPC) rolling horizon framework and grounds on the model as already presented in the confidential ELSA Deliverable 6.1 [2], compare section 2.3.1. The main difference to the service evaluation in ELSA Deliverable 6.1 is in the inclusion of the latest ELSA DT5 system and in the usage of a more sophisticated simulation modelling reflecting the German energy market conditions more adequately. This comprises, for example, the EEG (“Erneuerbare-Energien-Gesetz” – financial settlement according to the German Renewable Energy Law [13]) as pictured in the use case system design in Figure 10. An overview on the nomenclature used in Figure 10 is provided below.

- $P_{El_{PV.District}}$: Local PV power generation directly consumed by the city district
- $P_{El_{PV.Batt}}$: Local PV power generation stored by the ELSA storage
- $P_{El_{PV.EEG}}$: Local PV power generation directly sold to the EEG
- $P_{El_{Grid.District}}$: Grid power from the local energy supplier consumed by the city district
- $P_{El_{Grid.Batt}}$: Grid power from the local energy supplier stored by the ELSA storage
- $P_{El_{Market.District}}$: Power purchased from the energy trade market and directly consumed by the city district
- $P_{El_{Market.Batt}}$: Power traded on the energy trade market and charged or discharged by the ELSA storage
- $P_{El_{Batt.District}}$: Power discharged by the ELSA storage and consumed by the city district
- $P_{El_{Batt.EEG}}$: Buffered PV power discharged by the ELSA storage and sold to the EEG

To apply the participation to the national energy trade market use case to the Kempten district, three different products from the German EPEX energy spot market [14] are considered:

Product A) Day-ahead auction [15]

Product B) Intraday auction [16]

Product C) Intraday continuous [17]

In the following, the day-ahead auction product is denoted as product A, the intraday auction product as product B, and the intraday continuous product as product C.

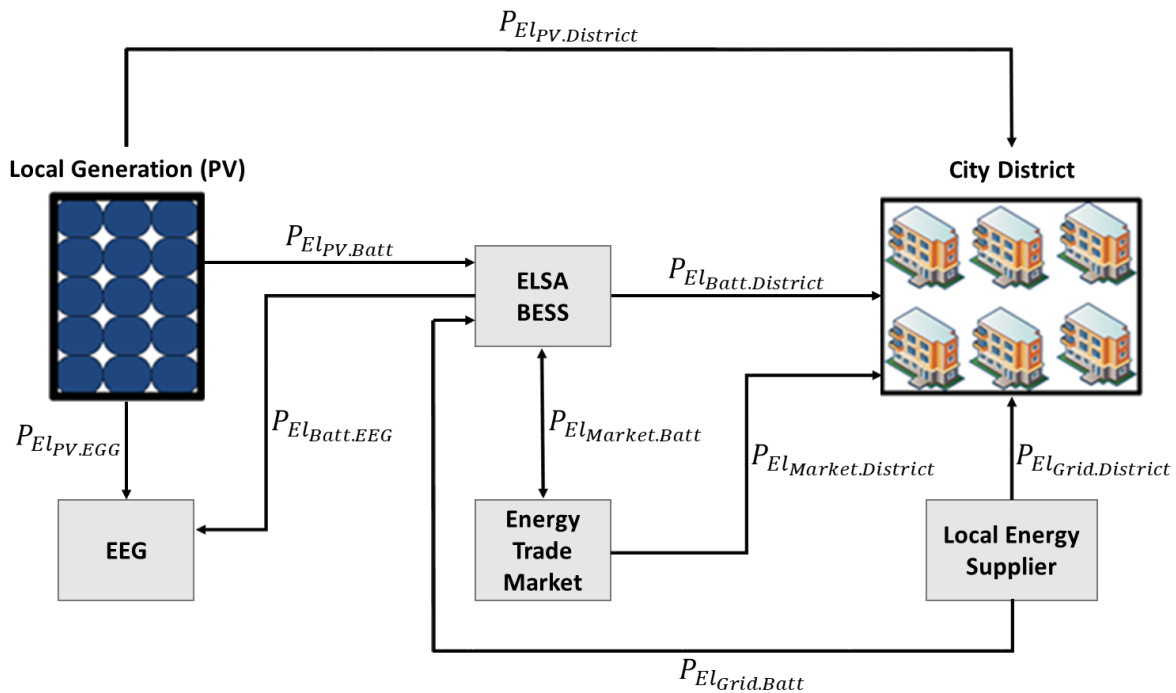


Figure 10: System design for the participation to the national energy trade market use case

For product A, the minimum volume increment is 0.1 MW per hourly energy block and the daily auction takes place at 12 a.m. for the 24 energy blocks of the successive day. For product B, the minimum volume increment is 0.1 MW per quarter-hourly energy block and the daily auction takes place at 3 p.m. for the 96 energy blocks of the successive day. For product C, the minimum volume increment is 0.1 MW per quarter-hourly energy block and the energy blocks can be traded continuously until 30 min before the delivery period begins. Starting at 4 p.m. daily, all energy blocks of the successive day can be traded for product C.

To participate to the national energy trade market, the minimum volume increments for those German spot market products would already exceed the physical ELSA storage capabilities in its present form installed at the Kempten pilot. For this reason, it is assumed that in total ten ELSA storage systems of type DT5 – each of them with the same capabilities of the current 66 kWh ELSA storage installation at Kempten – would operate as one aggregated BESS in order to enable this work the system level analysis of the intended use case. This leads to the technical parameters of the upscaled ELSA BESS as follows:

- Charging power range: 1.2 kW – 720 kW
- Discharging power range: 1.2 kW – 720 kW
- Battery storage capacity: 660 kWh
- Round-trip efficiency: 80 %

Furthermore, both the total power consumption of the Kempten district and its local PV power generation were rescaled by a factor of ten as well, so that the relative conditions between the upscaled ELSA BESS's capacity and the local district's power consumption/generation magnitudes remain in the same ratio. This assumption results in a power consumption base load of approximately 200 kW and in an installed PV peak power of 371 kWp for the Kempten pilot.

For the application of the use case, a Model Predictive Control (MPC) rolling optimization computes piecewise the schedule for the considered large-scale ELSA BESS within the MPC operation horizon $\mathcal{T} = [t, t+1, t+2, \dots, t+96], \forall t \in T$, where T is the overall simulation horizon. This means that one optimization is carried out for all $t \in T$ discrete time steps comprising in each case the next $\tau \in \mathcal{T}$ future time steps and one has to distinguish between two stages per optimization run as follows: The first stage is intended to identify the energy blocks for products A and B, which seem to be highly profitable, i.e., which offer cheap energy block prices for purchasing power, and which conversely offer high energy block prices for selling power. Thus, for each energy block it is necessary to predefine lucrative offers, which means maximum and minimum block prices for the purchasing or selling of power. For example, one simple method to determine these individual energy block offers is in the usage of a moving average filter over the historic energy block prices from the past weeks. However, more advanced forecasting techniques, e.g., using artificial neural network forecasting approaches, are imaginable as well. All the identified lucrative offers per energy trade market product are then communicated to the energy trade market and each of them can either be accepted or rejected based on the assumption that an offer can either meet or not meet the current energy block price that is declared in the auction. This is visualized in Figure 11 as a flow chart, where $\hat{T}_A \subset T$ denotes the set of gate closure time steps for product A, i.e., 12 a.m. every day, and where $\hat{T}_B \subset T$ denotes the set of gate closure time steps for product B, i.e., 3 p.m. every day. In the second stage and based on all the accepted energy block offers for products A and B per time step t , it is eventually optimized towards the minimum district operator's energy costs to supply for its district, which is done by solving a mathematical optimization problem as an extension of the mathematical optimization model presented in section 2.3.1. This optimization model also includes the determination of lucrative energy block offers for product C to be communicated to the energy trade market. An overview on the deployed optimization problem formulation is provided in Annex B.

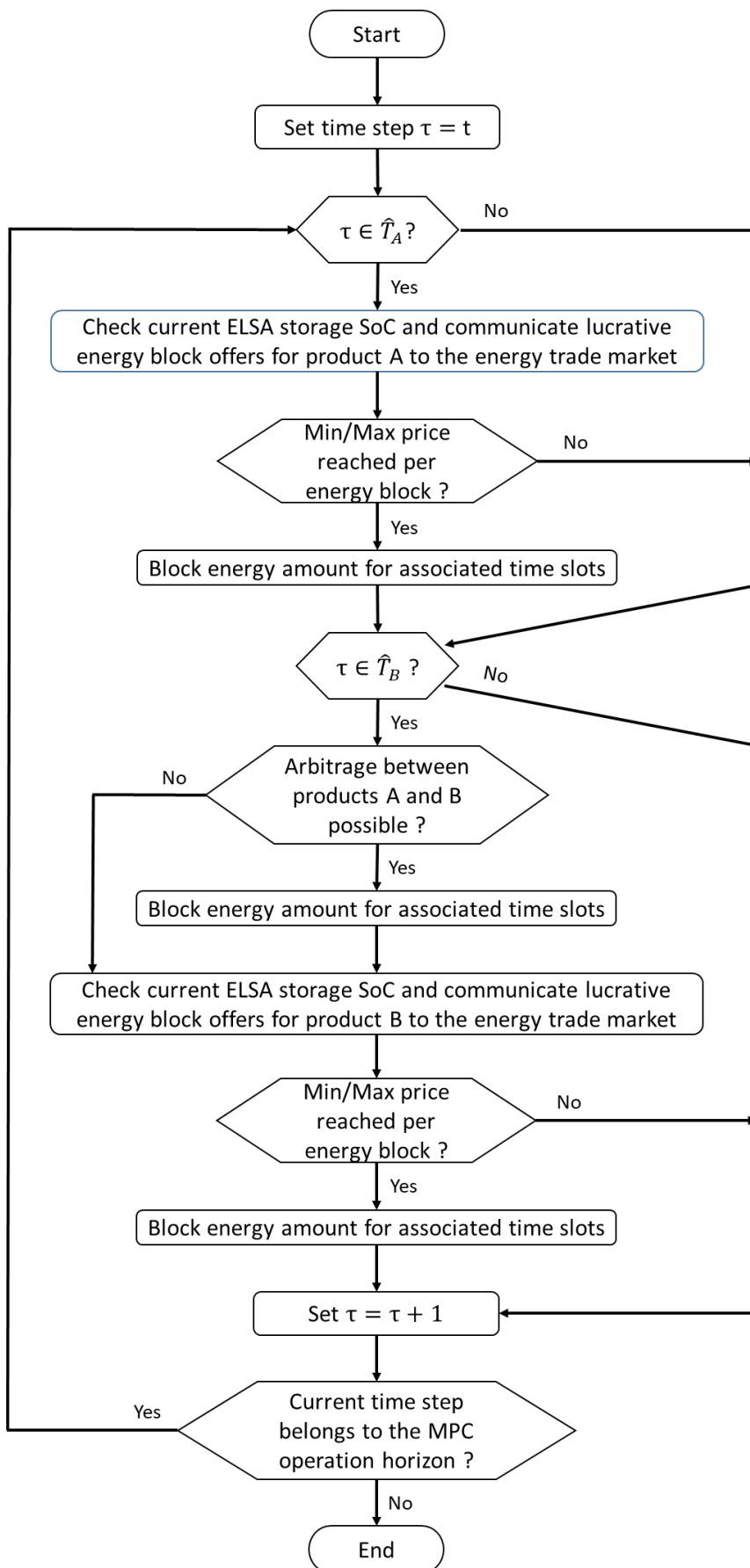


Figure 11: First stage of the MPC rolling optimization

3.3.2 Results

To evaluate the participation to the national energy trade market use case, the described optimization procedure in the previous section is applied to a typical summer week (July 31, 2017 until August 07, 2017). The upscaled power demand of the city district and the local PV generation within this summer week are shown in Figure 12. For the three different energy trade market products considered, real historic energy block prices are taken from [14]. On top, the different energy block prices C_{A_t} , C_{B_t} and C_{C_t} are assumed to already include energy market trading fees of 0.1593€ based upon the information provided in [18]. The grid tariff C_{Grid} is assumed to be 0.2866€ [19]. The reward for the EEG $C_{PV.EEG}$ is considered with 0.1028€ [20] and the reward for local PV power self-consumption by the district $C_{PV.District}$ is determined as 0.2056€, i.e., it holds $C_{PV.District} = 2 \cdot C_{PV.EEG}$.

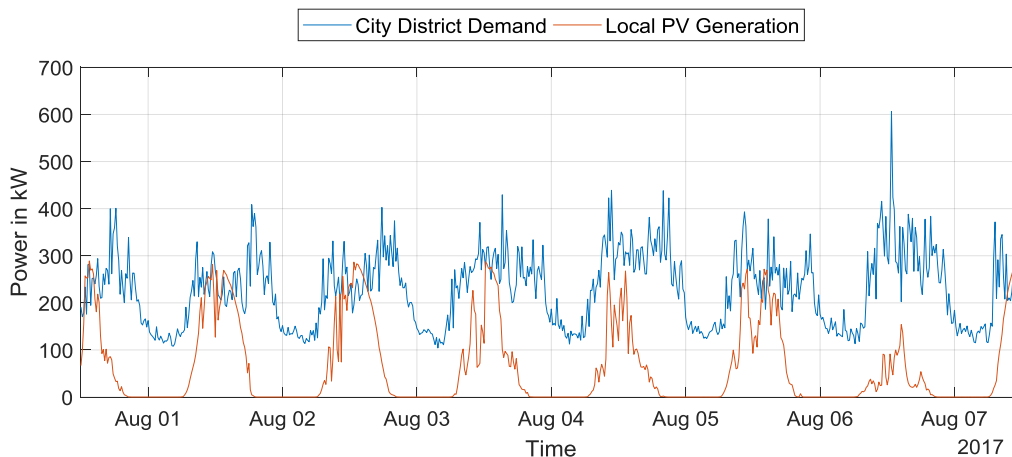


Figure 12: City district power demand and local PV power generation during the considered summer week

For the analysed summer week, Figure 13, Figure 14 and Figure 15 show the interaction with the different energy trade market products A, B and C. From these figures, it can be seen that most of the required energy to supply for the city district is purchased directly from the day-ahead market (product A), since it prevalently offers the cheapest energy prices compared to products B and C within the considered summer week. Moreover, it can be seen that there is barely any arbitrage between the three products because of the following reasons: First, the prices for the different energy trade market products usually possess a strong correlation with each other, which is why there are only little differences in the prices declared for a certain time step t . Second, the a-priori calculation of the lucrative energy block offers for products A and B does not primarily target arbitrage intents. Third, using the ELSA BESS for arbitrage purposes is not economically worthwhile, because its round-trip efficiency of 80% is too low. Fourth, compared to the grid tariff C_{Grid} of 0.2866€, it is in most cases more reasonable to let

the city district consume already purchased energy instead of selling it back to the energy trade market.

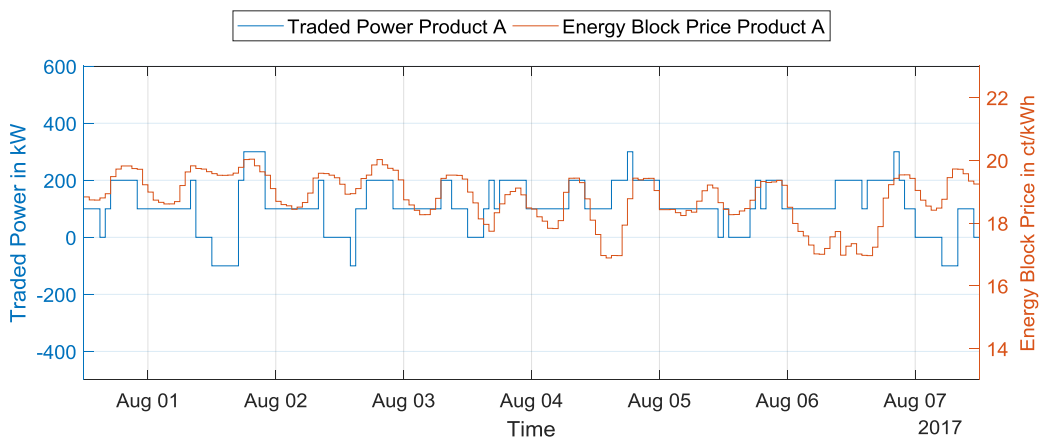


Figure 13: Traded power for product A during the considered summer week

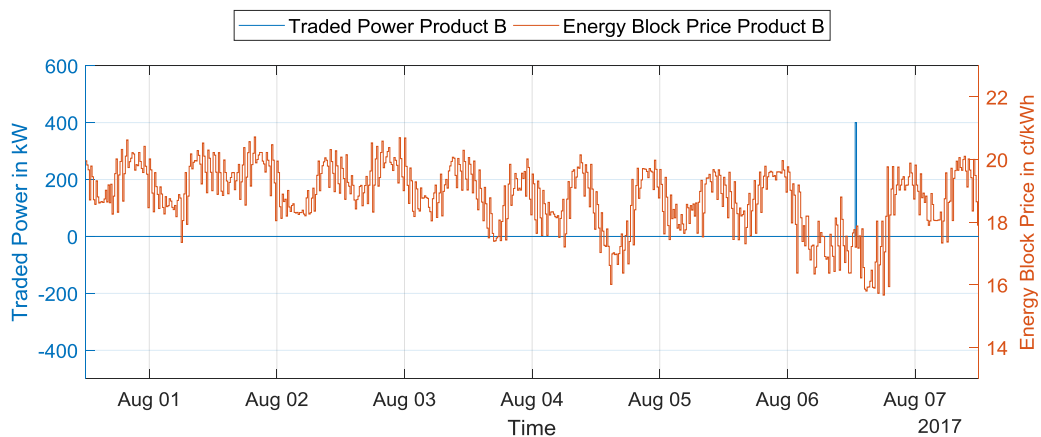


Figure 14: Traded power for product B during the considered summer week

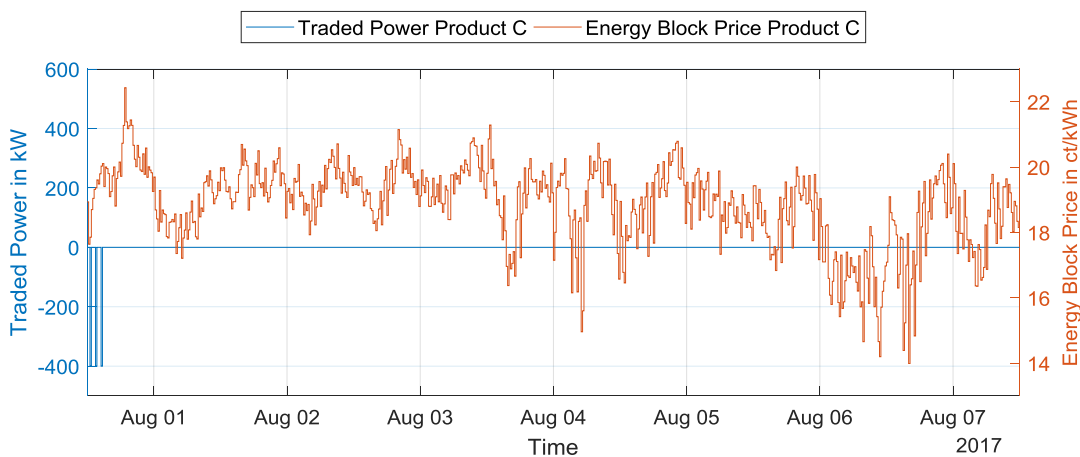


Figure 15: Traded power for product C during the considered summer week

However, under the consideration of the desired objective to decrease the overall energy costs for a district operator to supply for its district, the participation to the national energy trade market use case clearly brings a benefit. This can be deduced from Table 1, which provides an overview on both the total trading volumes for the different energy commodities as pictured in Figure 10 and the total energy costs for the district operator to supply for its district according to metric (3.1). Further and for the sake of evaluation, two different scenarios are considered in Table 1. For the first scenario, it is assumed that the upscaled ELSA BESS is installed at the city district and for the second scenario, it is assumed that no ELSA storage is installed at the city district. Thus, the scenario without ELSA BESS serves as a reference case here, where a participation to the national energy trade market is not possible. On that condition, it can be concluded from Table 1 that a district operator might save up to 1 675.83€ (28.7%) within a single summer week if the district operator is able to take advantage of a local ELSA BESS installation. This result is due to the fact that this use case scenario allows the district operator to actively participate on the national energy trade market which finally enables the district operator to benefit from cheaper prices for the purchase of energy in order to supply for its district. This decreases the volume of energy that is purchased from the (usually more expensive) local energy supplier by up to 18 052 kWh (64.3%). Nevertheless, since the main part of the city district's energy demand is covered by the energy trade market now, it is important to mention that the self-consumption of locally produced PV energy may decrease as well, but obviously this highly depends on the underlying tariffs $C_{PV.District}$ and $C_{PV.EEG}$.

Metric	With ELSA storage	Without ELSA storage (reference)
City district energy demand	38 631 kWh	38 631 kWh
Local PV energy generation	10 904 kWh	10 904 kWh
PV energy consumed by the city district	10 208 kWh	10 553 kWh
PV energy sold to EEG	696 kWh	351 kWh
Energy purchased from the local energy supplier	10 025 kWh	28 077 kWh
Energy purchased from the energy trade market	19 600 kWh	0 kWh
Energy sold to the energy trade market	1 200 kWh	0 kWh
District operator total energy costs	4 165.50 €	5 841.33 €

Table 1: Evaluation and comparison of the metric values for different energy commodities and the district operator's total energy costs during the considered summer week for a scenario with ELSA BESS and a scenario without ELSA BESS

3.3.3 Conclusion

The participation to the national energy trade market use case leads to reduced energy costs for district operators to supply for their districts, which makes it an attractive service to commercially use ELSA storage capabilities on the city district level. Additionally and from a system level perspective, the reduced energy costs for district operators might most certainly also affect the consumer energy tariffs within the city district and one can expect electricity price reductions for the customers. However, considering the overall operation costs, i.e., in the terms of the energy losses due to the ELSA storage system's low round-trip efficiency and the necessity for a large ELSA BESS installation in capacity and space, the net savings for the participation to the national energy trade market use case are expected to be rather low. For the achieved savings of 1 675.83€ for the simulated summer week, this finally would result in a saving of approximately 168€/BESS, which is rather small compared to the profits of the other large-scale use case applications, compare the subsequent sections.

3.4 Impact Analysis for Balancing Group Optimization

The balancing group optimization use case is based on the balancing group mechanism in the German energy market design and has also been presented in [21]. Balancing groups are used for the planning of generation and consumption of electrical energy. Every generator, consumer, and storage unit must be part of a balancing group. Based on a forecast or on standard load profiles, the generation and consumption is then forecasted, usually in a daily process for the next days. This aggregated forecast is then provided to the Transmission System Operators (TSOs) for grid operation planning purposes.

The balancing group manager must ensure that its group is always balanced; that is in each 15-minute-interval during a day. However, actual load and generation may deviate from the forecasts and thus, in actively managed balancing groups, these deviations are mitigated by intraday energy trading as shown in equation (3.6).

$$E_{imbalance,t} = E_{consumption,t} + E_{generation,t} + E_{sell,t} + E_{buy,t} = 0, \quad \forall t \in T \quad (3.6)$$

This allows the balancing group manager to continuously update forecasts, closer to the delivery time, to achieve a higher precision. Yet, as intraday trades are only possible until 5 to 30 minutes before the delivery period begins, there is still a risk of deviations. Depending on the direction of the deviation (excess or lack of energy) and the imbalance energy price (positive or negative), a positive or negative cost is linked to any imbalances in the balancing group.

These mechanisms result in two objectives for the balancing group manager as follows:

1. Reducing energy imbalances as requested by the TSOs. Heavy and regular imbalances can be penalized by the TSOs, potentially leading even to the withdrawal of the approval for a balancing group.
2. Reducing the imbalance costs as an economic requirement of the balancing group operation.

Depending on the current situation in a market area, different combinations of positive or negative imbalances and prices are possible, requiring different actions by the balancing group manager to fulfil the objectives stated above. Specifically, the actions as illustrated in Figure 16 might be taken into consideration by the balancing group manager in case of battery storage operations.

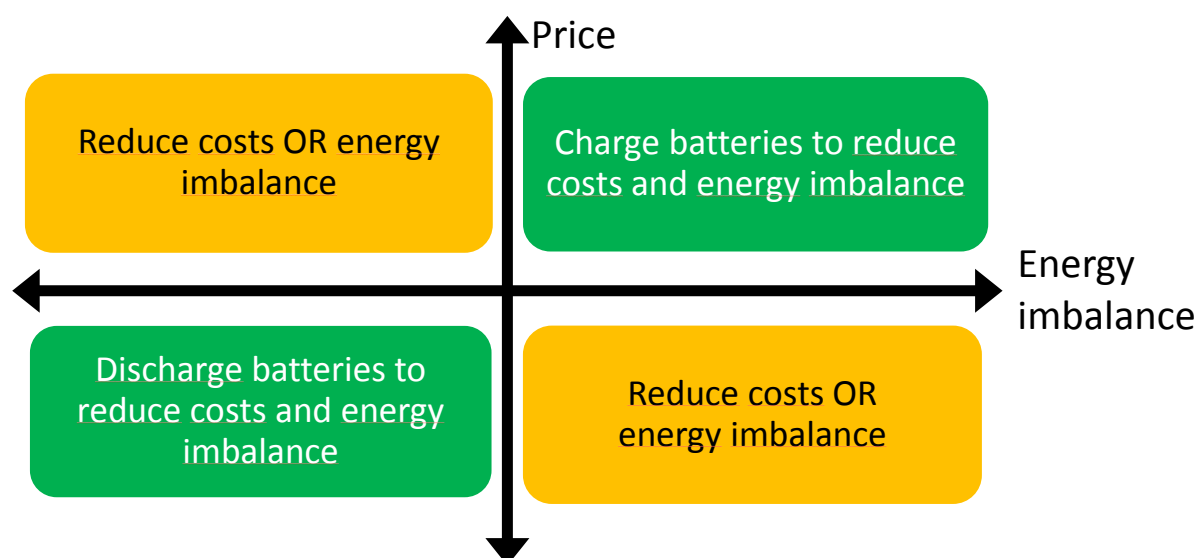


Figure 16: Battery storage operation depending on the balancing group situation

In Figure 16, a positive price denotes the additional costs for injecting power into the grid and a positive imbalance denotes the additional power that is being injected into the grid. In case of a positive price and an energy imbalance, the BESS can be charged to reduce both cost and energy imbalance for the balancing group. In case of a positive price and a negative imbalance, the BESS can either be charged to reduce costs and increase energy imbalances, or be discharged for the contrary effect.

3.4.1 Use Case Description

For the balancing group use case, different strategies were applied for the ELSA BESS operation, considering both objectives and the different situations that may occur in a balancing group as described in the previous section. The balancing group manager can either choose

to operate the BESS only in the “green zones” in Figure 16 to make sure that both objectives are fulfilled whenever the BESS is activated. However, this limits the potential of the BESS usage. Alternatively, the BESS can always be activated, optimizing either the cost or imbalance alone or for both objectives, ranked by their priority. The latter is known as the lexicographic method, a state-of-the-art multiobjective optimization strategy. In total, six different optimization strategies are considered, compare Table 2.

Optimization strategy	“posProd”	“simple”	“lexico”
Battery operation	Green zone	All zones	All zones
Optimization objective	Cost or imbalance	Cost or imbalance	Cost and imbalance prioritized

Table 2: Battery operation strategies for balancing group management

For the optimization strategies “posProd” and “simple” as shown in Table 2, either cost or imbalance reduction is chosen as the optimization objective, whereas for the “lexico” strategy, cost and imbalance are chosen and prioritized. The applied lexicographic method in the “lexico” strategy performs a first optimization for the primary objective. The result of this first optimization is then used as an additional optimization constraint in a second optimization for the secondary objective.

The objective functions for cost and energy imbalance reduction are provided in equations (3.7) and (3.8) where $E_{imbalance}^{residual}(t)$ is the residual energy imbalance and $Price_{imbalance}(t)$ is the related price.

$$\min \sum_{t=0}^T E_{imbalance}^{residual}(t) * Price_{imbalance}(t) \quad (3.7)$$

$$\min \sum_{t=0}^T |E_{imbalance}^{residual}(t)| \quad (3.8)$$

For the evaluation, data from a real balancing group managed by Allgäuer Überlandwerke GmbH (AÜW) [12] is used. More precisely, the available data, containing the energy imbalances and imbalance prices of one week in a 15-minute resolution, is used in an offline optimization to evaluate the potential of the ELSA system for the cost and energy imbalance reduction. The flexibility provided by the ELSA BESS is used to compensate energy imbalances as an alternative to imbalance compensation by energy trading.

In contrast to local use cases, the number of BESS units that can be used is less limited (e.g. by physical constraints). To evaluate the potential benefit of battery storage usage in the terms of the theoretical optimum of cost reduction and energy imbalance reduction, the optimization was performed for each of the six strategies described above, varying the number of ELSA BESSs from 0 to 150, where each single ELSA BESS has a capacity of 88 kWh, symmetric charging and discharging powers of 96 kW and a round-trip efficiency of 80%.

Due to the investigation of scaling effects, marginal benefits can be estimated for the usage of additional ELSA BESSs regarding the optimization objectives. The reference case to evaluate the different strategies uses no ELSA BESS; therefore, no flexibility is available for imbalance or cost reduction.

For the cost optimization, there is no lower limit. Costs can even be negative – in practice corresponding to earnings for the balancing group. The energy imbalance in the reference case is around 1.115 MWh with a theoretical lower limit of zero in the optimization, which would mean that the group is balanced in any time step.

3.4.2 Results

The imbalance costs for the different scenarios are shown in Figure 17.

The imbalance costs are negative in the reference case, where no BESS is used, as the existing imbalances correlate with beneficial imbalance prices for the chosen time interval of the balancing group. This effect purely results from the input data and not from the optimization or the applied strategies.

Applying cost optimization leads to a linear correlation between the number of ELSA BESSs and imbalance costs. For the cost-simple and cost-lexico scenarios, a cost decrease of about 800 €/BESS can be achieved over a horizon of one week. For the cost-posProd scenarios, cost decrease is only 300 €/BESS, as the batteries are only operated part-time and the full potential cannot be exploited. In all three scenarios, the BESS operation is based on using the imbalance price changes to generate profit by creating higher energy imbalances, which is not desired by the TSO and accordingly reflected in the balancing group agreement. The total energy imbalances are massively increasing in all three scenarios, as shown in Figure 18.

The subordinated optimization of energy imbalances in the cost-lexico scenario causes only a little improvement compared to the cost-simple scenario and a simultaneous minimization of costs and imbalances is not possible for these scenarios. This applies even to the cost-posProd scenario, which was supposed to prevent this effect. The failure of this strategy to decrease imbalances is caused by an overshoot behaviour, as the BESS not only charges to precisely compensate for positive imbalances, but charges with higher power than necessary, creating new, negative imbalances. The overshoot behaviour could be prevented by setting a limit for the BESS charging power according to the positive imbalance in a certain time period. The

same effect can also be observed for discharging and could be prevented by setting a limit for the BESS discharging power, too.

A focus on cost optimization is clearly beneficial from the economic perspective of the balancing group manager. From the perspective of the TSO, this behaviour must be prevented as higher unscheduled imbalances may jeopardize the stability of the power system.

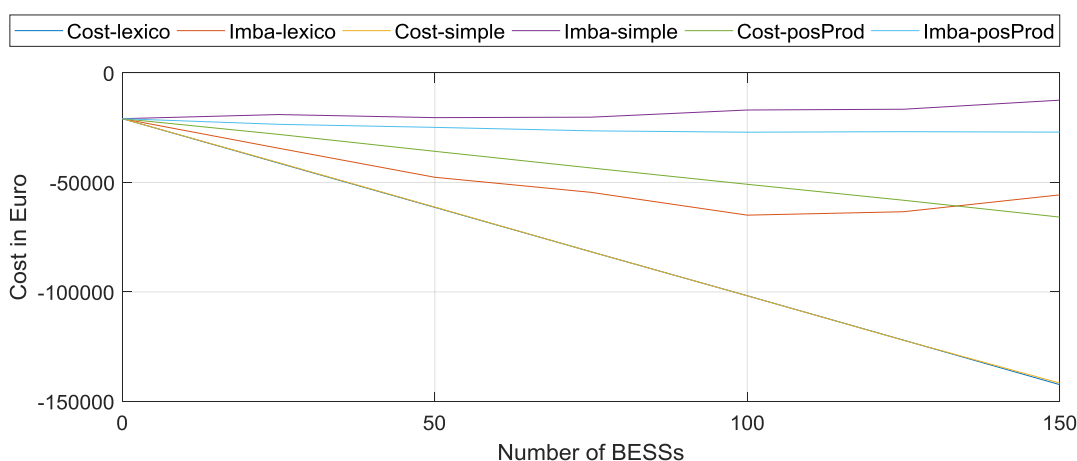


Figure 17: Balancing group management – cost objective

As shown in Figure 18, applying imbalance optimization leads to a decrease of energy imbalances of up to 226 MWh for the imba-simple and imba-lexico scenarios and up to 105 MWh for the Imba-posProd scenario. The correlation between the number of BESS and energy imbalance is not linear for any of the scenarios, resulting in a diminishing marginal benefit for imbalance optimization.

The effects on costs is diverse for all three scenarios. Costs are even increasing in the imba-simple scenario, which is reasonable as the imbalance costs are not considered therein. Imba-posProd is successful in the terms of preventing costs from increasing. Yet the cost decrease is small, there is only a minor financial incentive for applying this strategy. For the imba-lexico scenario, a significant decrease of costs can be observed with a cost minimum for approximately 100 ELSA BESSs.

From the economic perspective of the balancing group manager, imba-lexico strategy would be chosen with a maximum of 100 BESSs, providing the largest economic benefit of about 440 €/BESS. In this case, a decrease of energy imbalances of 115 MWh would be achieved, contributing to smaller deviations in the balancing group and accordingly to smaller fluctuations in the power system.

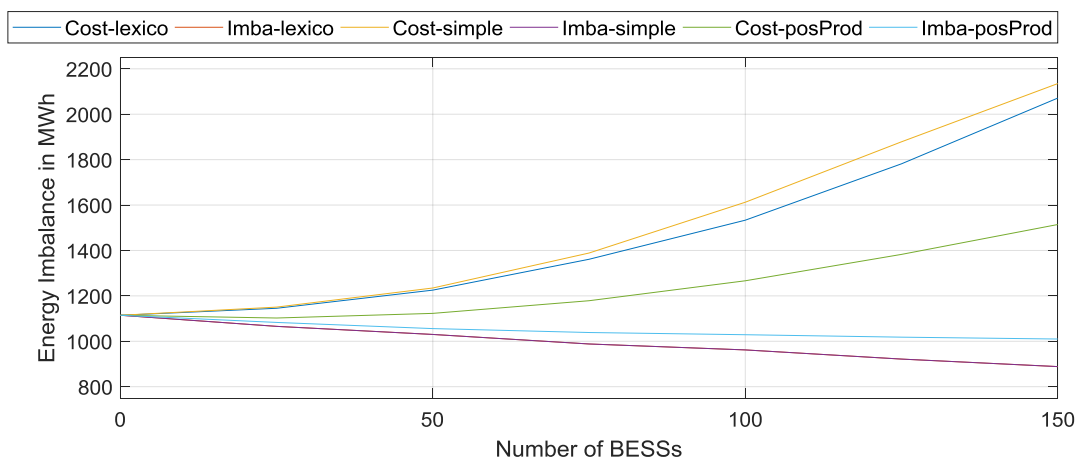


Figure 18: Balancing group management – imbalance objective

Rated power and capacity of the BESS are limiting factors with respect to the optimization objectives. The upscaling effects have been studied by increasing the number of BESSs in the optimization, thus keeping the ratio between rated power and capacity constant. For 150 ELSA BESSs, the total rated power almost reaches the peak power of the imbalances curve.

Therefore, there is barely any further benefit in increasing power for the imbalance scenarios. Instead, a higher total BESS capacity is needed, allowing the BESS the balancing over longer time periods. For the cost scenarios, additional BESSs would always provide a proportional cost decrease. Even though other limitations would occur in real applications, costs could theoretically be decreased up to the point, where the effect of the BESS usage would significantly influence the imbalance prices on the system level.

3.4.3 Conclusion

Due to the limited BESS operation range in the cost-posProd and imba-posProd scenarios, these ones cannot provide comparable benefits as the other strategies. For minimizing costs, the cost-simple and cost-lexico scenarios provide the greatest benefit, while the latter performs slightly better in the terms of energy imbalance reduction. Yet both strategies are substantially increasing imbalances and therefore are to be avoided from the TSO perspective. The imba-simple scenario, on the other hand, increases the costs for balancing group operators and hence is not of particular interest. Finally, the imba-lexico scenario reduces both costs and imbalances. Even if the cost reduction is smaller compared to the cost-simple and cost-lexico scenarios, imba-lexico provides a good trade-off and successfully satisfies both objectives.

3.5 Impact Analysis for Primary Reserve Control Participation

As described in section 3.4, balancing groups are used in the German electricity markets to balance the generation and consumption in the planning phase. Yet even with active balancing group management, aiming to reduce any energy imbalances by energy trading, the reaction will be too slow to immediately compensate for deviations in the very short-term horizon. Such short-term deviations can occur due to outages, faults or rapid changes of the weather conditions. To compensate for the imbalances in these situations, balancing power or control reserve is used by the TSOs.

The provision and activation of control reserve is structured according to the following three stages:

- **Primary control reserve** is provided by all synchronously connected TSOs in the ENTSO-E [22] area according to the solidary principle. It is automatically activated, requiring a complete activation after 30 seconds and covering the first 15 minutes after any frequency deviations occur.
- **Secondary control reserve** is used to secure the energy balance in a control area and to control the frequency. It is automatically activated by the TSO of the respective control area and requires full activation 5 minutes after it is requested.
- **Tertiary control reserve** or minute reserve is activated by the TSOs to cover the time interval between 15 minutes and one or several hours after an incident occurs. It must be completely activated after 15 minutes.

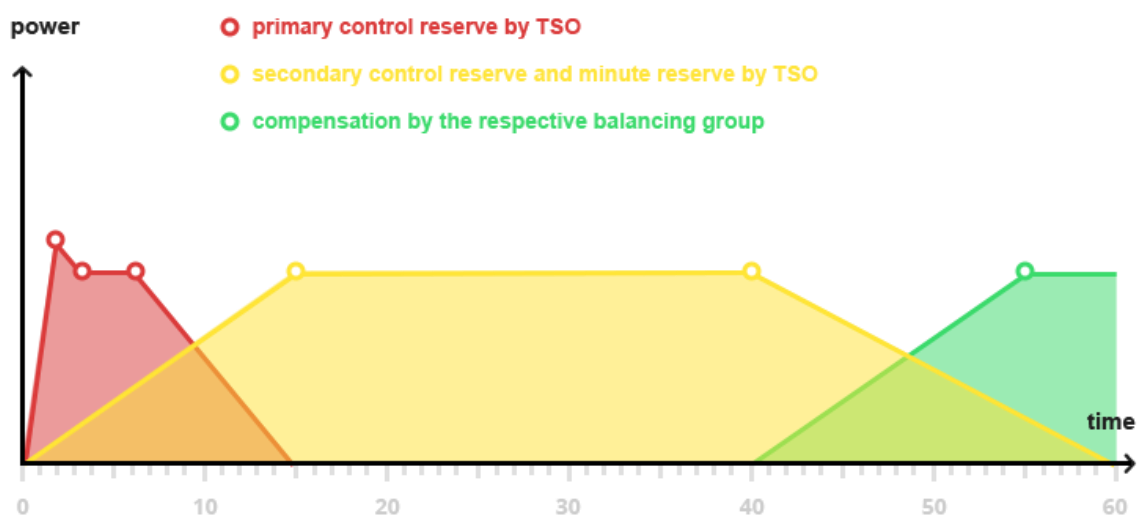


Figure 19: Principle of control reserve utilization in the German market, Source: [23]

As shown in Figure 19, the different stages of control reserve are covering the interval from the occurrence of an incident until the compensation is feasible by market mechanisms, i.e., intraday trading.

Each of the control reserve products described above is auctioned in a daily or weekly process by the TSOs. Participating in these auctions requires a “prequalification” of the participant and of its IT infrastructure as well as of its “technical units”, i.e., generation, storage or consumption units that provide flexibility for control reserve operations. In the past, control reserve was provided by large power plants only, but the market was gradually opened for other participants, including smaller technical units by aggregating them in so-called Virtual Power Plants (VPPs). From the TSO perspective, these VPPs can then provide the same services as conventional large power plants. In parallel, the control reserve markets were also opened for storage units, e.g., battery storage. Thus, even for relatively small batteries, participation in control reserve is possible by aggregation to a VPP to exceed the minimal power that must be offered, which is 1 MW for primary control reserve (symmetrically in both directions) and 5 MW for the other two products (either positive or negative flexibility).

As prices are still most attractive for primary control reserve, battery usage is typically concentrated on this product, leveraging on fast reaction and high gradients that are provided by battery storage systems. However, the requirements to availability of control reserve are high, which has to be considered especially for batteries due to their limited capacity.

Different requirements must be considered for the usage of BESSs for primary control reserve applications. The primary requirements for batteries are related to the available power that can be offered and to the permitted SoC range during normal operation as follows:

- It is not allowed to offer the total rated power of a BESS to the primary control reserve market. Instead, 25% of the offered power must be available as a reserve for recharge strategies. This corresponds to 80% of the rated power of the BESS available to be offered to the market.
- It has to be guaranteed during normal operation that the offered power is available for at least 30 minutes. This limits the SoC range for the battery operation and subsequently increases the need for applying recharge strategies to keep the BESS in the permitted SoC range.
- If larger frequency deviations occur, the operation of the BESS out of the permitted SoC range is allowed. However, the BESS must return to the normal operation range within at most two hours.

The power request for primary control reserve directly depends on the frequency deviation from 50 Hz, requiring the following behavior for BESSs:

- In a dead-band of ± 10 mHz, no action is required from the BESS.

- In-between ± 10 mHz and ± 200 mHz, the requested power is proportional to the frequency deviation and the available power is fully requested for a frequency deviation of +200 mHz (charging BESS) or -200 mHz (discharging BESS), respectively.
- If the deviation is larger than ± 200 mHz, the available BESS power is fully requested.

3.5.1 Use Case Description

For the ELSA BESS based on the DT5 system, the parameters as stated in Table 3 were used in the simulation.

Parameter	Formula symbol	Value
BESS rated power	$P_{BESS,rated}$	96.0 kW
BESS available power	$P_{BESS,available} = 0.8 * P_{BESS,rated}$	76.8 kW
BESS reserve power available for market transactions	$P_{BESS,reserve} = 0.2 * P_{BESS,rated}$	19.2 kW
BESS rated capacity	$E_{BESS,rated}$	88.0 kWh
Normal operation – maximum SOC	$\frac{E_{BESS,rated} - 0.5 h * P_{BESS,available}}{E_{BESS,rated}}$	0.564
Normal operation – maximum SOC	$\frac{0.5 h * P_{BESS,available}}{E_{BESS,rated}}$	0.436

Table 3: BESS parameters for the ELSA DT5 system in the primary control reserve context

To allow for the operation of the BESS in the permitted SoC range, different recharge strategies can be implemented.

Overfulfillment of requested primary control reserve is permitted up to a limit of 120% as shown in Figure 20, which can be systematically used to increase the charging or discharging power if there is a charge or discharge request. Yet it must be noted that underfulfillment is not permitted.

In the **dead-band for small frequency deviations** of up to ± 10 mHz as shown in Figure 21, the BESS may also be activated to systematically charge or discharge itself. The requirements to the BESS operation are the same as in the normal operation range of ± 10 mHz to ± 200 mHz, i.e., the requested power is proportional to the frequency deviation and an overfulfillment of up to 120% is permitted.

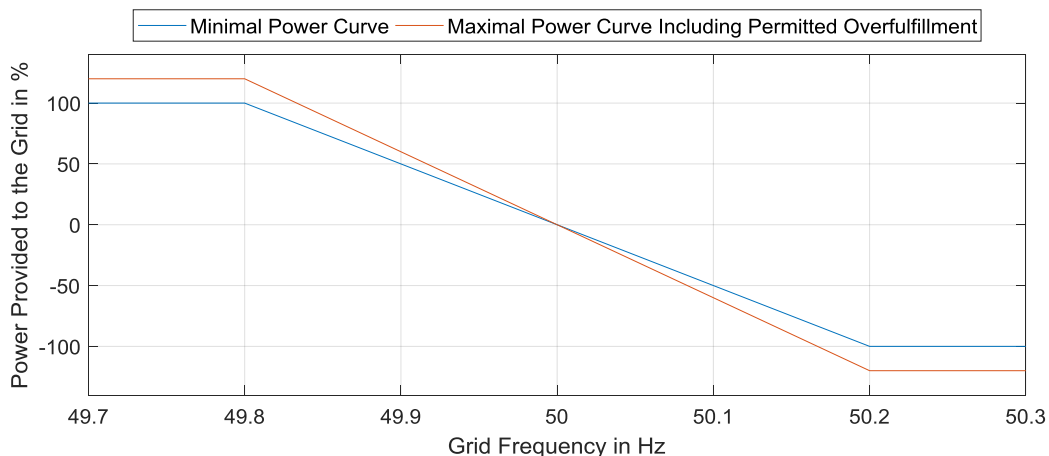


Figure 20: Primary control reserve - optional overfulfillment, Source: Adapted from [24]

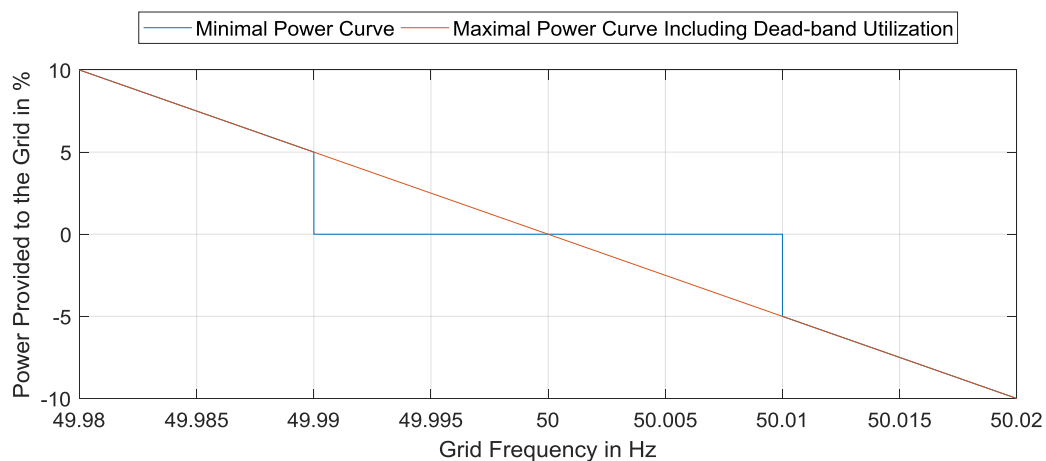


Figure 21: Primary control reserve – dead-band usage, Source: Adapted from [24]

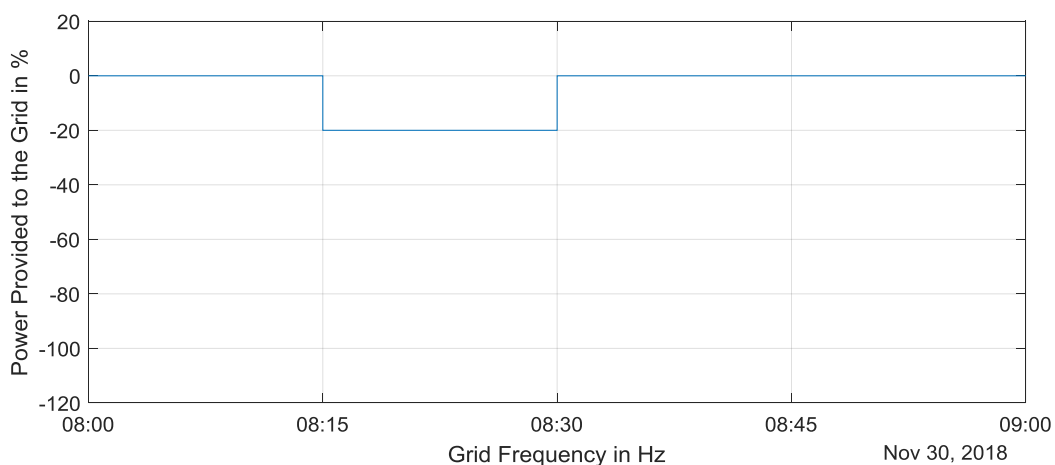


Figure 22: Primary control reserve – market transactions, Source: Adapted from [24]

Market transactions can be used to compensate for long-term charging and especially discharging of the BESS as shown in Figure 22. It is important to mention that the required power reserve for a BESS is dedicated to recharging strategies, meaning that 20% of the rated power of the system must be available for this purpose at all times.

The priority of the battery operation for primary reserve power is to maximize the available power that can be auctioned, i.e., to avoid leaving the allowed SoC range. To keep the SoC in the desired range, a combination of the recharge strategies named above can be applied. In this analysis, the following scenarios are considered:

1. No recharge strategy as the reference scenario, showing the SoC behavior over one week and indicating the need for recharge strategies. It is assumed that the requested primary control reserve is always delivered, while the BESS is not charged or discharged in the dead-band.
2. Systematic overfulfillment and dead-band exploitation for small frequency deviations, as these can be applied automatically and do not require energy trading, minimizing the necessary effort in the operation. The utilization of the options is simply based on the SoC of the BESS, additionally charging the BESS for a SoC below 50% and discharging it for a SoC above 50%. The requested primary control reserve is therefore delivered to 100-120%, while in the dead-band 0-120% primary reserve power is delivered. Different thresholds may be set in practice based on individual needs.
3. Compensation by market transactions according to simple rules based on the SoC deviation from a predefined target SoC. As in the first scenario, it is assumed that the requested primary control reserve is always delivered, while the BESS is not charged or discharged in the dead-band.

All scenarios are evaluated for one week (January 29, 2018 until February 04, 2018) and are compared in regard to their capability to maintain the desired SoC range. While this cannot be guaranteed for the first two scenarios, it turns out that this is always possible in the third scenario.

For the decision about market transactions in the third scenario, the rules are provided in equations (3.9) – (3.11).

$$SoC_{deviation_t} = SoC_{operation_t} - SoC_{target}, \forall t \in T \quad (3.9)$$

$$P_{BESS,charge_t} = \max \left(\frac{SoC_{deviation_{t-1}} * E_{BESS,capacity}}{0.25 h}, -P_{BESS,reserve} \right), \forall t \in T \quad (3.10)$$

$$P_{BESS,discharge_t} = \min\left(\frac{SoC_{deviation_{t-1}} * E_{BESS,capacity}}{0.25 h}, P_{BESS,reserve}\right), \forall t \in T \quad (3.11)$$

The economic benefit of the primary control reserve participation is not depending on the requested power or energy, but only on the available power of the BESS. If the desired SoC range can always be maintained, the benefit B can be calculated from the available power as presented in section 3.2.3.

3.5.2 Results

As it can be seen from Figure 23, the desired SoC range can only be maintained in the third scenario, including energy trading in the recharge strategy, as the compensation by overfulfillment and the exploitation of the dead-band is not sufficient. For the first and second scenario, the SoC quickly drops below the minimum SoC of 43.6% due to energy losses during charging and discharging operations. If these losses are not compensated by energy trading, the BESS would be completely discharged leading to an interruption of the provision of the control reserve.

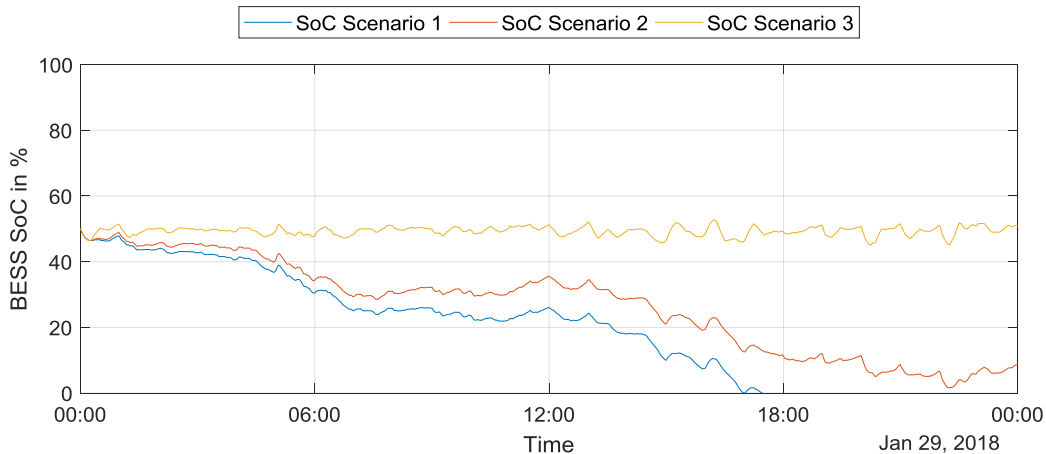


Figure 23: BESS SoC for the three different reserve control scenarios

Figure 24, Figure 25 and Figure 26 show the power requested during primary control reserve participation over the course of one day as well as the deviations caused by different recharge strategies. In all scenarios, heavy fluctuations of the power output can be observed, reflecting fluctuations of the grid frequency. The power output for scenario 1 is slightly lower compared to scenarios 2 and 3. The power output is zero while frequency deviations are in the dead-band, as no recharge strategies were applied in this scenario. For scenario 1, this should lead to lower stress on the BESS due to high ramps and sudden load changes compared to the other two scenarios. Nevertheless, a highly dynamic behaviour is required from the BESS for primary

control reserve participation compared to other use cases. This can also be observed in comparison to the power curve of market transactions, i.e., traded energy, which was applied as recharge strategy in scenario 3.

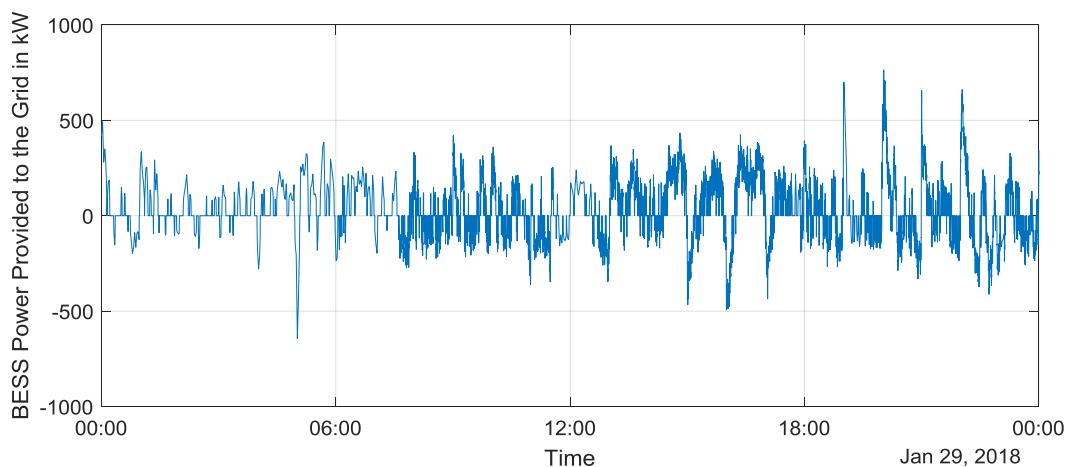


Figure 24: BESS power provided to the grid for scenario 1

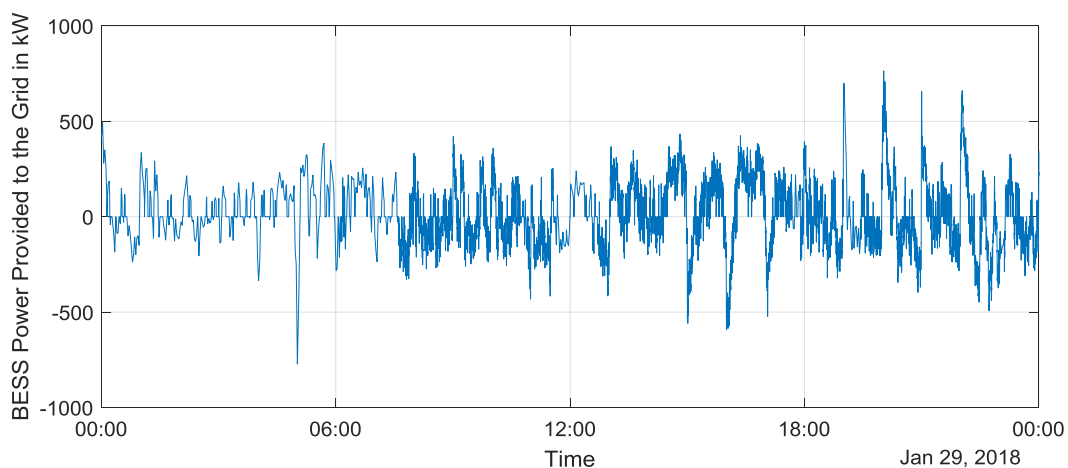


Figure 25: BESS power provided to the grid for scenario 2

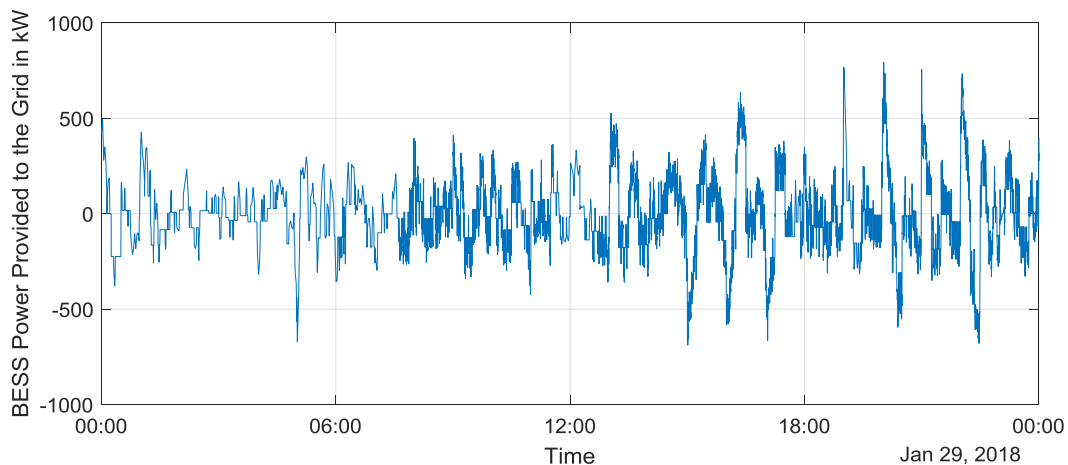


Figure 26: BESS power provided to the grid for scenario 3

Due to an increasing number of battery storage systems and aggregated small generation units participating in primary control reserve, prices have declined over the last years as shown in Figure 27 and it is assumed that this trend is continuing according to [25].

Still, an average weekly profit of 2 452€/MW or 188€/BESS could be achieved during the year 2017. In 2018, the average weekly profit was 2 026€/MW or 156€/BESS between January and October.

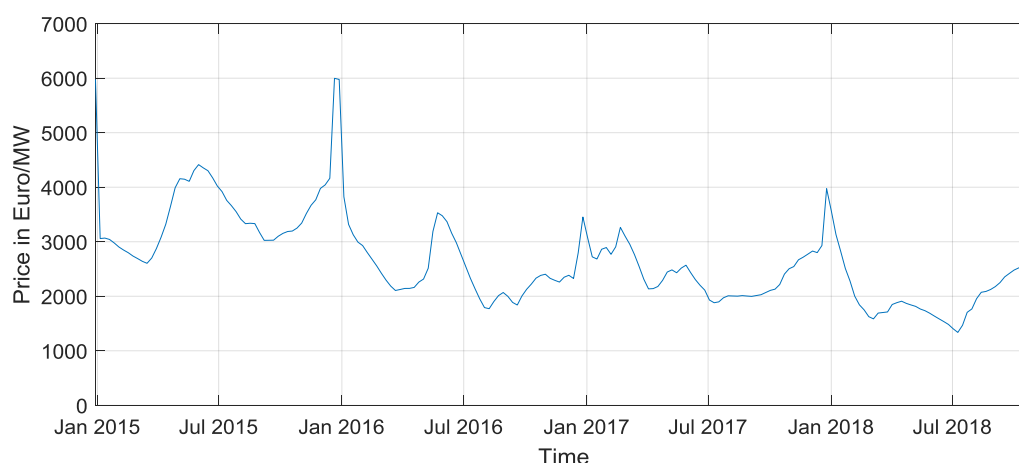


Figure 27: Primary control reserve price trend

3.5.3 Conclusion

Primary control reserve participation with maximized available power is only possible in combination with intra-day market trading for the compensation of long-term losses or extreme frequency deviations, as described in the previous section. This effect is assumed to be even more critical in a real application, where additional effects such as self-discharging of the BESS occur and which have not been considered in this study for the sake of simplification. However, higher efficiency in charging and discharging as well as a higher capacity in relation to the available power will decrease the need for energy trading. To decrease the capital expenditure (CAPEX) and operational expenditure (OPEX) per BESS due to energy trading, multiple ELSA BESSs should be aggregated, providing the additional benefit of increasing the reserve for any faults or outages of BESS and providing additional flexibility in the bidding process of the primary control reserve auctions.

3.6 Use cases comparison

It has been shown in the previous sections that with an upscaled ELSA BESS, additional use cases become feasible and economically viable. The required total BESS power and capacity, however, highly depends on the actual use case, ranging from up to 10 BESSs for the national

energy trade market use case to 15 – 20 BESSs required to provide the requested minimum power of 1 MW for the primary control reserve participation with sufficient reserve in case of BESS failures. Usage of battery storage in a balancing group and (apart from the regulatory requirements) participation in primary reserve control is not requiring a certain minimum number of BESSs. However, a cost decrease is to be expected by upscaling the system, as fixed costs for infrastructure and trade market access can be shared by a higher number of BESSs. Moreover, both the capacity-specific price for lithium ion batteries and the power-specific price for the power electronics is expected to decrease within the next five years, compare Figure 28. Currently, the ELSA BESS price is estimated at approximately 580 €/kWh.

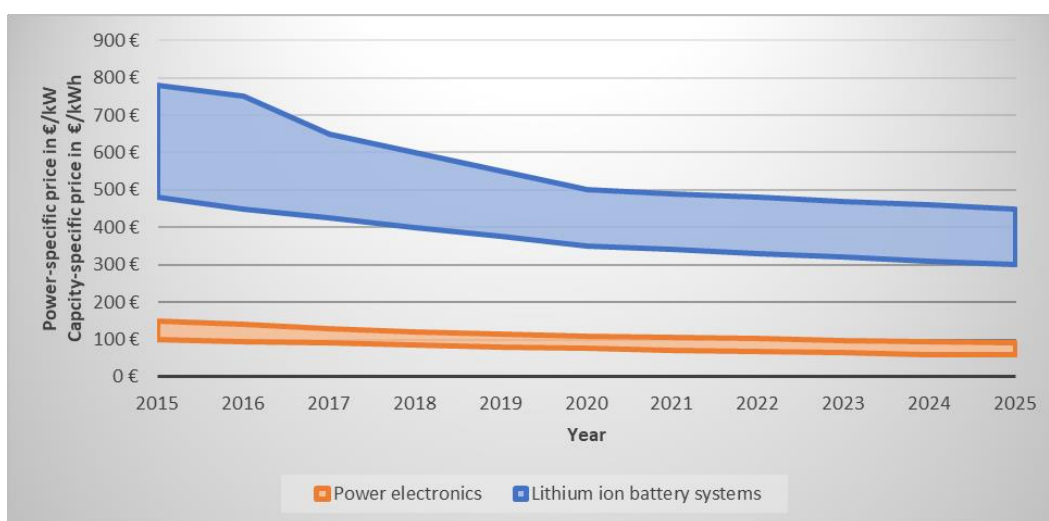


Figure 28: Price development for lithium ion battery systems and power electronics, Source: Adapted from [26]

A comparison of the different use cases is provided in Table 4, where the “-”, “o” and “+” signs indicate a low, average and high dynamicity or cost, respectively.

Use Case	Estimated weekly profit	Required dynamicity	Expected cost
Participation to the national energy trade market	168 €/BESS	-	o
Balancing group optimization	440 €/BESS	o	o
Primary control reserve	156 €/BESS	++	+

Table 4: Comparison of the potential for the different large-scale use cases with upscaled BESS

Considering the estimated weekly profit provided in Figure 4, the net present value of the profits over the economic life of a BESS can be calculated. In Figure 29, the net present value

for the different use cases is shown for an adequate target rate of 12.5%. For the investment costs, a price goal of 580 €/kWh has been assumed with a rated capacity of 88 kWh per ELSA BESS. This costs do not include consulting, integration of the ELSA BESS and its platform, and the Energy Management System (integration and aggregation of the ELSA BESSs). Further, operating costs are not considered here.

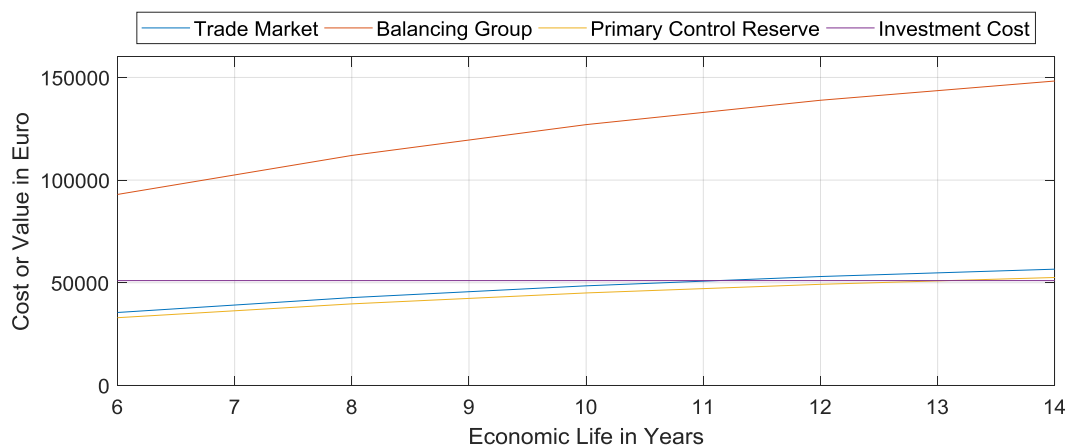


Figure 29: Investment cost and profit value for different use cases

The comparison of profit value and investment cost highlights that the value of the investment is highly depending on the use case. With the assumptions given above, an economic lifetime of more than eleven and 13 years is required for the participation to the national energy market and the primary control reserve, respectively. For the balancing group optimization however, even with a lifetime of less than 6 years, the investment may provide a positive net present value. Yet it must be noted, that for an investment decision, a more detailed calculation is required, including e.g. operating and integration costs and price developments of the products in respect to the relevant use cases.

4 HiL Simulation

4.1 Introduction

In order to understand the control of multiple ELSA BESS aggregated to one large-scale system, it is necessary to understand and test the limits of the communication infrastructure. Since it is not feasible to set up and interconnect 50 or more ELSA BESS in one system for cost as well as for space reasons, in this project a HiL approach has been chosen to investigate the capability of the communication infrastructure in a setup that combines real Device Under Test (DUT) and a scalable simulation. A HiL setup always consists of a simulation connected to a real hardware, as depicted in Figure 30. The main goal is to stimulate the connected hardware DUT with a controlled set of input signals. The DUT then reacts to the input signals and the outputs are fed back into the simulation. With this approach it is possible to investigate the behaviour of black box systems, but also of highly nonlinear systems with a large set of internal states. The overall setup consists of three major parts and one visualization tool, depicted in Figure 31, as follows:

1. The Coordinated Controller (CC) that will calculate the power set-points for each ELSA BESS, based on an external power demand signal. This is the real DUT.
2. The Real-Time Simulator (RTS), to simulate a limited number of ELSA BESSs in the electrical domain. The electrical simulation is necessary to produce meaningful data for the third block, which is the communication Simulation Computer (SC).
3. The communication SC will be able to start multiple, i.e., up to hundreds, of Intelligent Electronic Devices (IEDs) to provide the CC with different numbers of simulated ELSA BESSs.

During the tests, the CC will be challenged with varying numbers of ELSA BESSs, simulated within the communication simulation. The major goal is to determine the time needed from the moment a new power demand set-point is set at the CC and the moment the inverters in the (RTS) see a change in their set-points. The whole setup combines different domains, which need to be interfaced, namely electrical simulations, communication simulations, analogue signals, and Ethernet communication. This results in two major challenges.

First, the implementation of a reasonable good performing simulation for the communication is a prerequisite. In this context, the only feasible way is to introduce threads for each simulation, which results in a complicated communication between sub-threads and the orchestrator thread. And second, the triggering and synchronization from the DUT and RTS needs to be taken into consideration.

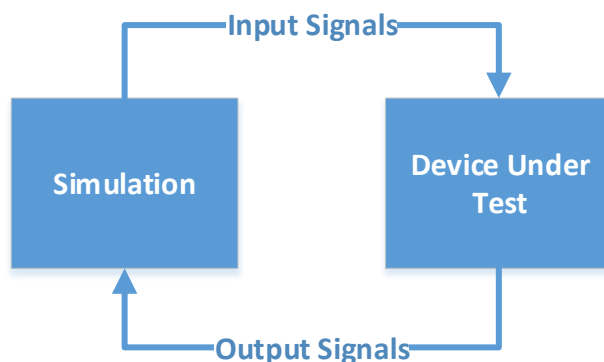


Figure 30: HiL schema

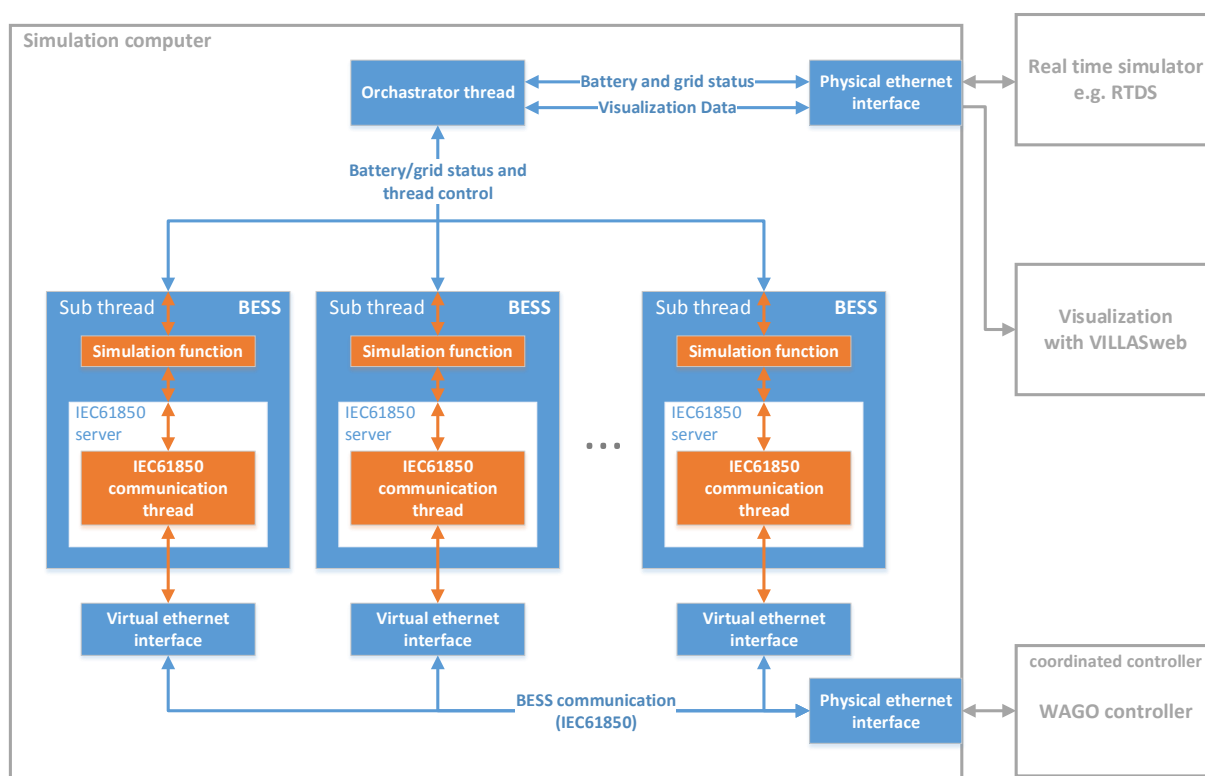


Figure 31: HiL system setup

4.2 Overall HiL Setup

4.2.1 Communication Simulation

The communication simulation is a software written in C++ and C since these languages support all the required functionalities and are compatible to a variety of hardware platforms, including the server running the simulation. The software provides an interface to the real-time simulation, the CC as well as, for visualization purposes, to VILLASWeb (see section 4.2.3).

In a first step, the software starts a control and an orchestrator thread. This routine thereafter can start a user-defined amount of sub-threads. Each of the sub-threads represents one BESS and each sub-thread can run one independent IEC61850 server plus a simulation function. This simulation function can, in the simplest case, transfer data between the orchestrator thread and the IEC61850 server or even run user-defined simulation functions in order to support the RTS system. Since the aim of Task 6.4 is to investigate the scalability of identical systems from a design perspective, all the IEC61850 servers are started with the same definition file and all the sub-threads are loaded by the same simulation routine. The simulation functions as well as the IEC61850 server run on independent memory and cannot interact with each other, except through the orchestrator thread or the CC.

The communication between the communication SC and the CC is realized via TCP/IP. One individual IP address is assigned to each of the IEC61850 servers. All the IP addresses are bound to one physical interface to which the CC is connected. The starting address is given as a parameter consisting of the first two bytes as the base address, whereas the third and fourth byte must be set individually. This results in a theoretical address pool of 65536 IP addresses that one can address. The final required parameter is the number of IEC61850 servers that are meant to be run. In combination with each IEC61850 server, there is one simulation function running that controls the IEC61850 server. The developed software was successfully tested with 1 000 simulated IEC61850 servers.

The communication between the communication SC and the RTS is defined by the protocol used by the RTS, which is UDP in this case. One data package from or to the RTS can hold up to 300 numbers. Each number can either be of type integer or float. The format needs to be predefined on both sender and receiver side. The communication SC can send and receive data from the RTS. The routine for sending and receiving of data is implemented in threads that run in parallel to the orchestrator thread, see Figure 31, which enables the communication to be performed independently from the orchestrator thread. Each simulation thread sends an update of its simulation status to the orchestrator thread in a predefined interval. The orchestrator thread then forwards that data to the RTS or to VILLASWeb.

4.2.2 IEC61850 Server

The IEC61850 standard [27] was originally specified to define the communication inside a power grid substation. The standard defines the overall design process from planning to implementation. For this task, only the implementation part is of importance. Based on the standard, there are three methodologies that can be used for communication. First, there is Goose, designed for low latency communication on an Ethernet level. Second, the standard defines Sampled Values (SV), which is intended to be used for data acquisition. In the current version of the standard, SV is available on the Ethernet level only. The third type of communi-

cation is Manufacturing Message Specification (MMS). MMS is intended to be used for routable control communication. This type of communication was selected to be used in the project, to provide a flexible and standardized interface for control purposes. To provide the IEC61850 server in the communication simulation, an open source implementation of the C library libiec61850 [28] was modified and a C++ interface to libiec61850 was developed.

In the IEC61850 standard, a server is defined by an IED Capability Description (ICD) file. This file describes a hardware in an XML format.

The main modification to the libiec61850 library is in the way such a server definition file is loaded. The workflow in the original libiec61850 library is as follows:

1. Load the ICD file
2. Convert the ICD model to static C model code
3. Compile the target project with the static C model code

This design flow results in recompiling the communication simulation every time a change in the ICD file is made. Furthermore, it would be necessary to predefine the number of simulated BESSs, before completing the communication simulation. This would result in an inflexible software design and would be time-consuming when changing the simulation setup for different measurements. To avoid this issue, an ICD parser, based on the libxml2 library [29] has been implemented. During the software initialization, the ICD file is loaded and directly parsed to create the memory model, needed by the libiec61850 library. This approach allows the user for the simple modification of the ICD file and only a restart of the software becomes necessary.

4.2.3 VILLASWeb User Interface

VILLASweb [30] is part of a software bundle developed at RWTH Aachen University in connection with different projects. Its aim is to provide a unified interface to different real-time simulators, including RTDS. In connection to this project, VILLASweb is used for visualization purposes during development. A screenshot is shown in Figure 32. The screenshot is taken during the communication testing and shows a transition between 5 kW and 500 kW output power. Furthermore, it is possible to control the simulation from the VILLASweb frontend and to set, for example, the SoC or the output power.

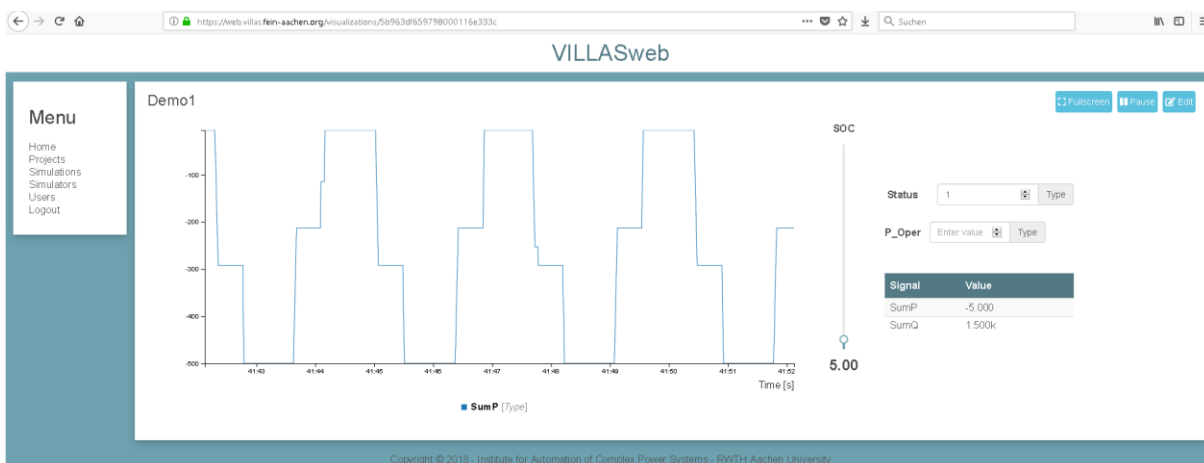


Figure 32: VILLASweb user interface

4.2.4 Controller DUT

In the architecture of the large-scale BESS, a hierarchical control scheme for multiple BESSs is applied as shown in Figure 33. The local controller monitors and manages the Power Converter System (PCS), while the CC acts as a second level of control, aggregating the BESSs towards a local master controller and running specific functions such as the power allocation, which is the focus of the scalability test. For the communication between the CC and the local master controller, the IEC61850 standard is used.

The functionality of the CC is implemented on a Wago controller, which is a Programmable Logic Controller (PLC). Hence, in the proposed HiL setup, the PLC acts as the DUT.

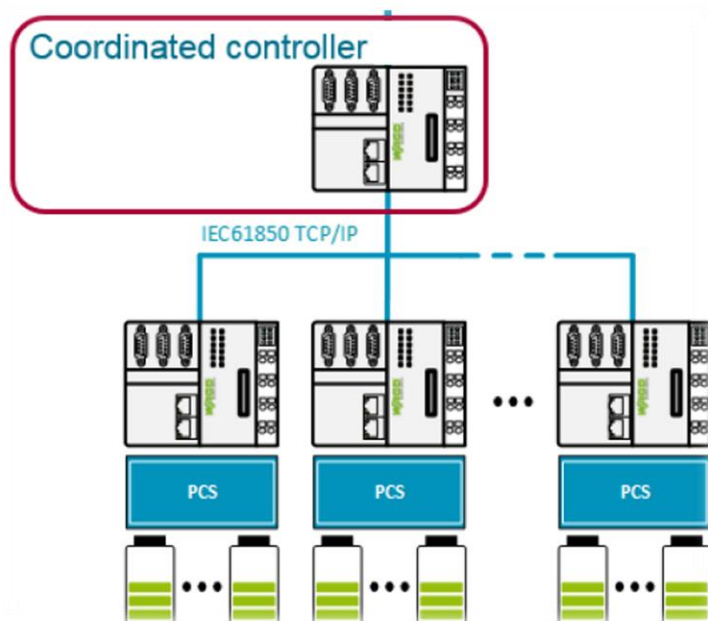


Figure 33: Architecture of a large-scale BESS

As aforementioned, power allocation is one of the main functions of the CC. Hence, a power allocation algorithm that calculates the power set-points for every BESS is implemented on the CC, according to [31]. The objective of the power allocation algorithm is to ensure a power balance. At the same time, it has to prevent the limits of the charging and discharging power of the BESS to not be exceeded.

The flowchart of the power allocation algorithm for the active power control is illustrated in Figure 34.

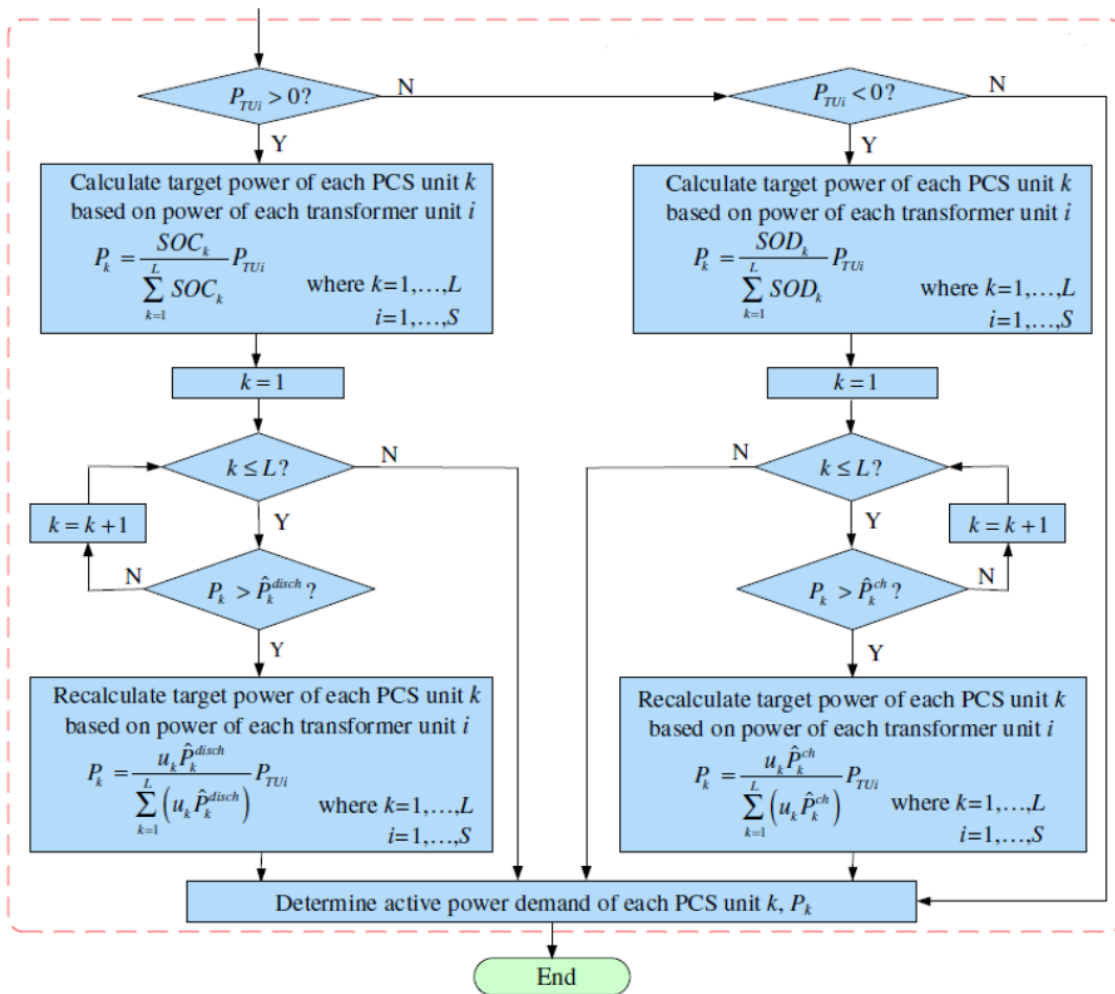


Figure 34: Flowchart of the power allocation algorithm for the active power control, Source: [31]

In Figure 34, SOC_k , SOD_k are the BESS's SoC and State of Discharge (SoD) respectively and u_k is the BESS status. L is the number of available BESSs, P_{TU_i} is the total active power demand and \hat{P}_k^{disch} , \hat{P}_k^{ch} are the BESS's maximum discharging and charging power, respectively.

In addition to the calculation of the active power set-points, the power allocation algorithm also calculates the reactive power set-points. The reactive power of each BESS Q_i is limited by

the maximum allowable reactive power \widehat{Q}_i , which depends on the maximum allowable apparent power S_i of the power converter system and the current operating power point of the BESS P_i , see equations (4.1) and (4.2). In equation (4.2), Q_{TUi} denotes the total reactive power demand.

$$\widehat{Q}_i = \sqrt{S_i^2 - P_i^2} \quad (4.1)$$

$$Q_i = \frac{u_i \widehat{Q}_i}{\sum_{i=1}^L (u_i \widehat{Q}_i)} Q_{TUi} \quad (4.2)$$

In order to run the described power allocation algorithm, the CC receives the status from the communication simulation software, i.e., the SoC and the operating power for each BESS, and in turn sends the calculated set-points to the SC. For the communication between the CC and the communication SC, the MMS transfer protocol running over the TCP/IP stack operating over the Ethernet, is used for the client/server services according to the IEC61850 standard. The CC acts as the client, meanwhile the multiple BESSs emulated in the communication simulation are the servers.

In order for the CC to read data from the remote servers according to the IEC61850 standard, the IEC61850 Solution tool offered by Wago [32] is used for setting up the MMS communication for the CC as a client. The tool imports the server capability description file to get the server configuration; then the MMS communication for the client can be set up.

It is worth noting that the IEC61850 communication needs a major part of the controller CPU power. Thus, according to this configuration, where the communication is established and maintained for the whole time between the client and servers, the maximum number of possible simultaneous server connections to the client is limited to 55 servers with 92.4% memory usage for the specific controller used (Wago 750-8206 [33]). Consequently, if the large-scale system, for example, should include 400 BESS, then 8 CCs are needed, where each CC manages 50 BESS and aggregates them towards the master controller.

Another implementation is the sequential connection approach. In contrast to the previous approach, the client connects to the servers sequentially now. In other words, there is only one connection at a time in order to read or write data. Hence, the client does not maintain the connection to the servers for the whole time. Once all inputs are available, the CC executes the power allocation algorithm and then connects sequentially to each IEC61850 server to update the power set-points, then disconnects and after that moves on to the next server.

These two approaches are explained in more detail in section 4.3. Additionally, the communication performance of the two approaches is investigated in section 4.5.

4.2.5 CC to RTS Communication and Trigger

A real-time communication link is established between the RTS and the communication simulation implemented in software. In particular, the socket protocol is used to send and receive UDP packets. The UDP packets received by the RTS contain the power set-points calculated by the CC. The UDP packets sent by the RTS contain the SoC, the status and the power operating set-points of the BESSs.

Moreover, to evaluate the communication performance of the large-scale system, the RTS is used for measuring the response time needed to set a new power reference set-point in the BESS.

The time measurement is triggered upon receiving an analogue signal from the CC at the point in time when a certain power demand is requested and stopped upon receiving the calculated power-set points from the communication simulation. Hence, the response time measurement includes the time required for running the power allocation algorithm in addition to the overall communication latency.

4.3 Test Conditions for Case Studies

The testing considers two different approaches for the communication between the CC and the BESS. The CC is represented by the embedded controller and the BESS by the simulated IED devices. The difference between the two case studies is made by the connection handling. In the first case study, the connection is opened, then data are read or written, and afterwards the connection is closed again. The second approach opens the connection to all simulated BESS instances and keeps it open. If triggered, the data is read or written.

4.3.1 Case Study 1

This case study describes the sequential approach. In this approach, the CC iterates through the different BESSs. In each iteration, the connection to one BESS is established, the data is read or written and the connection is closed. After all BESSs are read and written, the power allocation algorithm is executed, and then the BESS are accessed again. This procedure is illustrated in Figure 35.

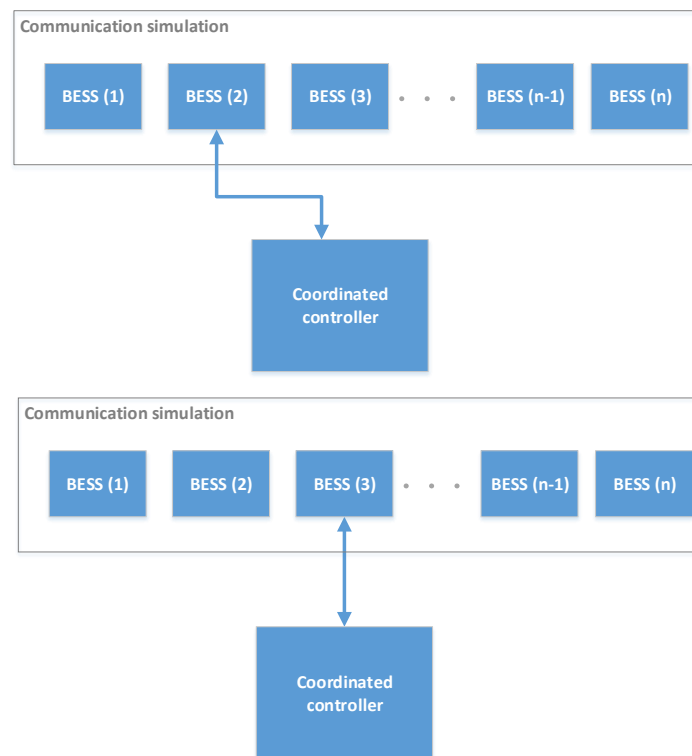


Figure 35: Case study 1 – Sequential approach with active connections (first, access to BESS (2); then access to BESS (3))

This approach reduces the required memory amount significantly, since the CodeSys development environment [34] instantiates one entire IEC61850 client for each connection on the CC. Moreover, this approach only requires one instance. To connect to the different BESSs, the IEC61850 server's IP address of that one instance is changed in every iteration. In addition to the memory needed for the IEC61850 instance, memory for storing the current values from the BESS and for the power allocation algorithm is required. Because of the advantage in memory usage, this approach can handle significantly more BESSs than the parallel approach. Unfortunately, the additional time for connecting and disconnecting in each iteration needs to be considered. The time required to read and write all BESSs increases linearly with the number of BESSs.

4.3.2 Case Study 2

This case study describes the semi-parallel approach to connect to the different simulated BESSs. As illustrated in Figure 36, the connection is established once by the CC, shown as dashed grey lines. When a read or write command is executed on the CC, the connection becomes active (blue line) and the command is executed, as depicted for BESS (2) in Figure 36. After all BESSs are read and written, the power allocation algorithm is executed and the BESSs are accessed again.

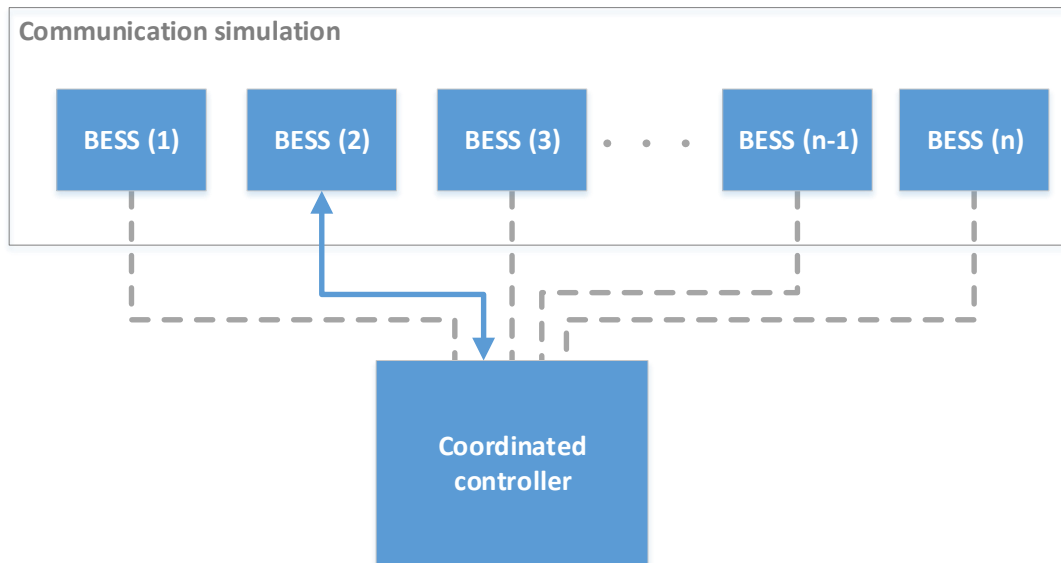


Figure 36: Case study 2 – Semi-parallel BESS access (active connection to BESS (2) and idle connection to the other BESS)

This type of connection handling reduces the time overhead for establishing and closing the connection. For this reason, it is faster in writing or reading values from the different BESSs. Unfortunately, this means that the CC has to handle n open connections simultaneously, which means that the controller needs n instances of the IEC61850 client in total. This increases both the required amount of memory and the network load. This poses a problem, since the used CC is limited to 16 MB of program memory (for the implemented CodeSys programme). This limitation of memory results in a maximum of 50-60 connections that can be handled by the CC. The supplier of the CC, however, recommends to use at most 20 connections [35].

4.4 System Characterization

The overall delay consists of different components, some introduced by software and others by hardware. To be able to assess the results of the overall delay measurement, the delay for each component needs to be examined. In the following paragraph, the individual delays of the communication between the RTS and the communication SC is investigated. Based on that, the system is extended with the CC to measure the latency induced by the sequential IEC61850 communication as described in section 4.3.1. Furthermore, the parallel approach as described in section 4.3.2 is analysed. Additionally, a network switch is added between the CC and the SC, to investigate the delay induced by the network infrastructure. Finally the power allocation algorithm is executed on the CC to represent the entire setup. On these grounds, the overall setup is evaluated in chapter 4.5.

4.4.1 Hardware and Setup Description

To test the use cases described in section 4.3, a sufficient hardware setup has to be built. The general setup contains a switch, the RTS, the communication SC, and the CC. The connection setup of those four components is shown in Figure 40. As the switch, a HP ProCurve 1800-24G [36] is used. This is a standard Ethernet switch. For the communication SC, a Dell PowerEdge R440 [37] with two Intel® Xeon® Silver 4114 CPU [38], see Figure 37, and 160 GB of DDR4 ECC RAM and an Intel X710-T4 Ethernet card [39] is used. The CC is represented by a WAGO 750-8206 PFC200 [33], see Figure 38.



Figure 37: Dell PowerEdge R440 SC installed at the RWTH Aachen pilot

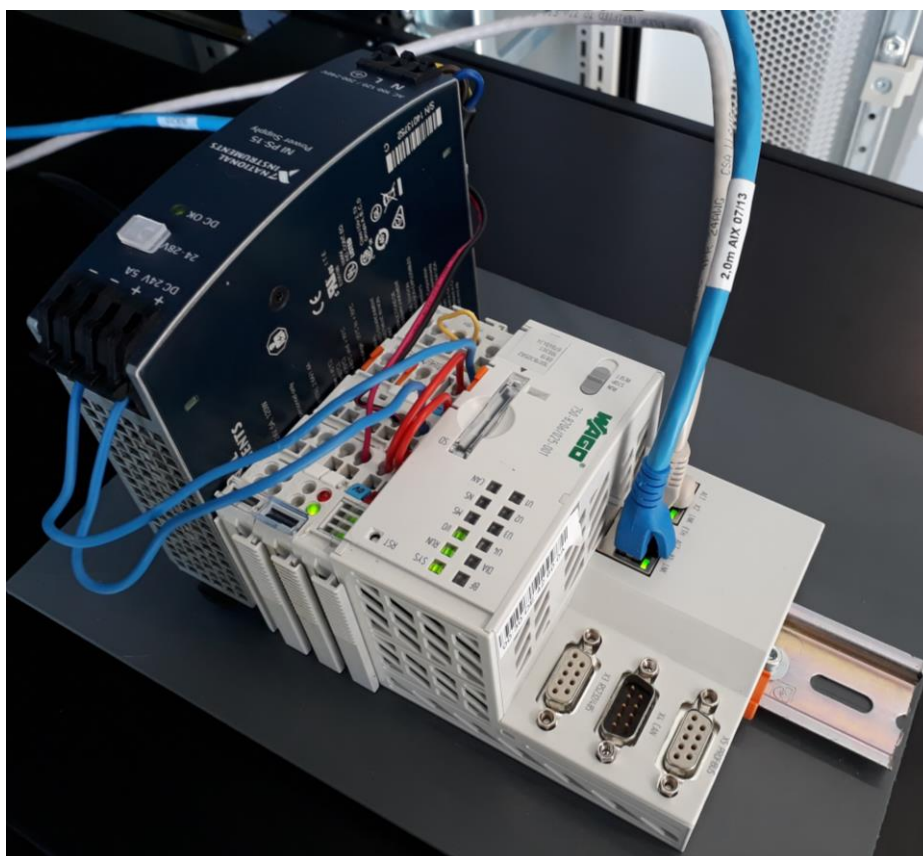


Figure 38: WAGO 750-8206 PFC200 installed at the RWTH Aachen pilot

To identify the delays induced by the different components in the setup, it is necessary to measure the setup in two configurations. First, the setup is connected as pictured in Figure 39. Second, the setup is modified by adding the network switch (Figure 40). The latter represents the “real-world” scenario, where multiple BESSs are interconnected by at least one network switch.

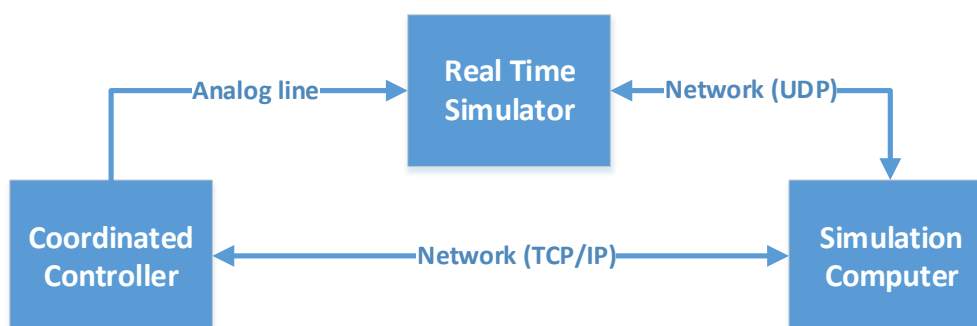


Figure 39: General test setup without switch

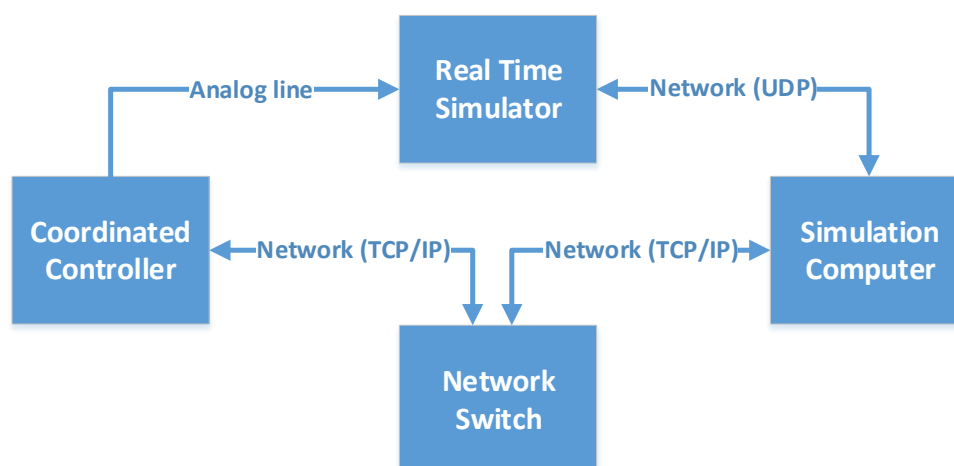


Figure 40: General test setup with switch

4.4.2 Connection Characterization RTS and SC

To test the communication between the RTS and the SC, a benchmark case is analysed. For this purpose, the RTS increments one integer number with a user-defined frequency. This number is sent to the communication SC. The communication SC then distributes this number to all running simulation threads. The simulation threads loopback the number to the orchestrator thread. When the value is received from all simulation threads, the orchestrator thread sends back the number to the RTS. The time elapsed between sending the number and receiving the number is measured in the RTS. Since the behaviour is depending on the number of simulation threads, this test will be done for different numbers of simulation threads. The

precision of the latency measurement is defined by the simulation step size of the RTS, which is set to 50 μ s.

Based on the results, the induced delays and limits of the RTS to the communication SC and the inter-thread communication can be quantified for different configuration parameters of the communication SC.

The test is performed with different configurations as listed in Table 5. The “Number of threads” is the number of simulation threads that run in parallel. The “Simulation time step” is the duration of one simulation step. The “Send interval” is the maximum amount of simulation steps until the simulation thread sends the current simulation status to the orchestrator thread. The “CPU overcommitment” is defined as the ratio between available CPUs and threads. In this setup, 48 CPUs including hyperthreading are available.

Configuration	Number of Threads	Simulation time step	Send interval	CPU overcommitment
5 fast update	5	50 μ s	50	0.10
50 fast update	50	50 μ s	50	1.04
500 fast update	500	50 μ s	50	10.42
5 slow update	5	500 μ s	50	0.10
50 slow update	50	500 μ s	50	1.04
500 slow update	500	500 μ s	50	10.42

Table 5: Configuration for characterization of connection between RTS and SC

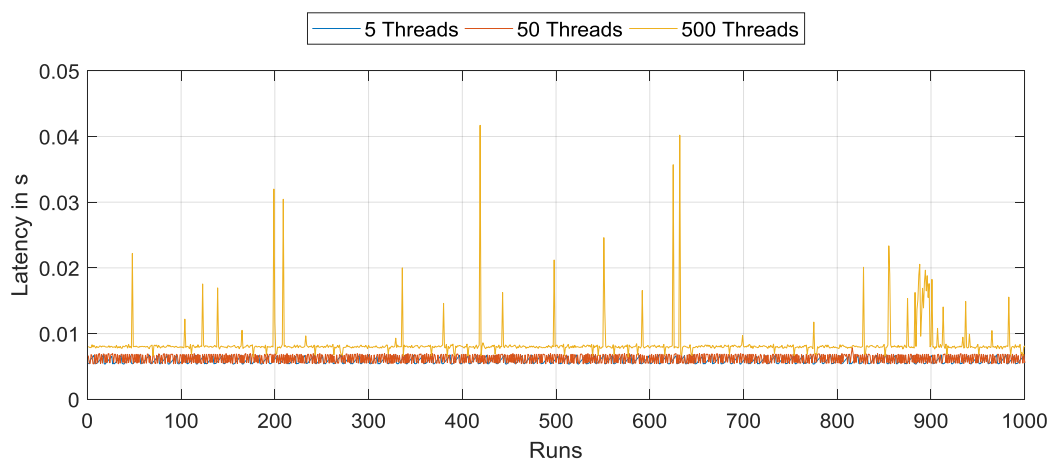


Figure 41: Fast update rate RTS to SC communication

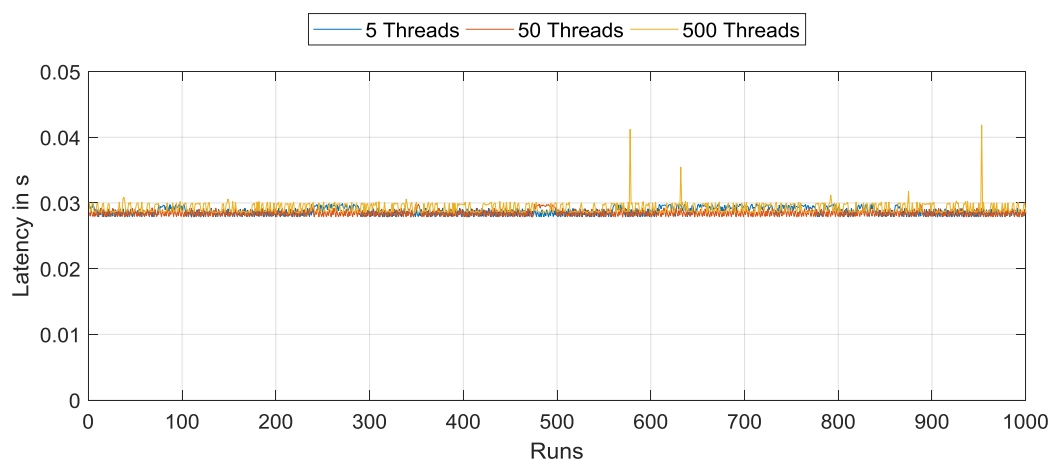


Figure 42: Slow update rate RTS to SC communication

The measurement results for 1000 simulation runs are shown in Figure 41 and Figure 42. The statistics for the measurements is shown in Table 6. It can be seen that with 500 threads the outliers are high compared to the 50 and 5 threads measurements, where no outliers can be identified. The number of outliers decreases, when the update rate between the simulation threads and the orchestrator thread is reduced, as it can be seen from comparing the yellow measurement curves in Figure 41 and Figure 42. The outliers can be explained with overcommitment of the CPUs as listed in Table 5. Based on these measurements, the following test will be done with up to 50 simulation threads at a fast update rate of 50 μ s and up to 500 simulation threads with a slow update rate of 500 μ s.

Configuration	Runs	Mean [ms]	Median [ms]	Max [ms]	Min [ms]	Standard deviation [ms]
5 fast update	5 734	5.9	5.9	6.9	5.3	0.43
50 fast update	5 047	6.2	6.7	11.3	5.3	0.65
500 fast update	4 182	8.4	8.0	49.9	6.4	2.9
5 slow update	1 064	28.7	28.7	29.9	27.8	0.58
50 slow update	1 070	28.5	28.4	29.8	27.8	0.47
500 slow update	1 038	29.2	28.8	41.9	28.3	0.84

Table 6: Statistics characterization RTS to SC communication

4.4.3 Connection Characterization Analogue CC to RTS Connection

To synchronize the CC and the RTS for time measurement, it is necessary to send a trigger signal from the CC to the RTS. For this trigger signal, a WAGO 750-559 analogue output block [40] is used. Based on the datasheet, it is known that this hardware has a 10 ms delay between setting a new analogue output in software and actually starting to rise at the output. Unfortunately no rise time is provided in the datasheet, which is why the rise time has to be measured manually. The measurements are shown in Figure 43. The rise time is 24.88 ms and the fall time is 25.92 ms. Since in the RTS the rise and fall time is considered, by specifying the trigger level for starting at 1 V and for stopping at 5.5 V, this delay can be neglected. Furthermore, for the tests where the on time is used, the rise and the fall time can be considered as a constant time offset and do not change the overall result of the measurement.

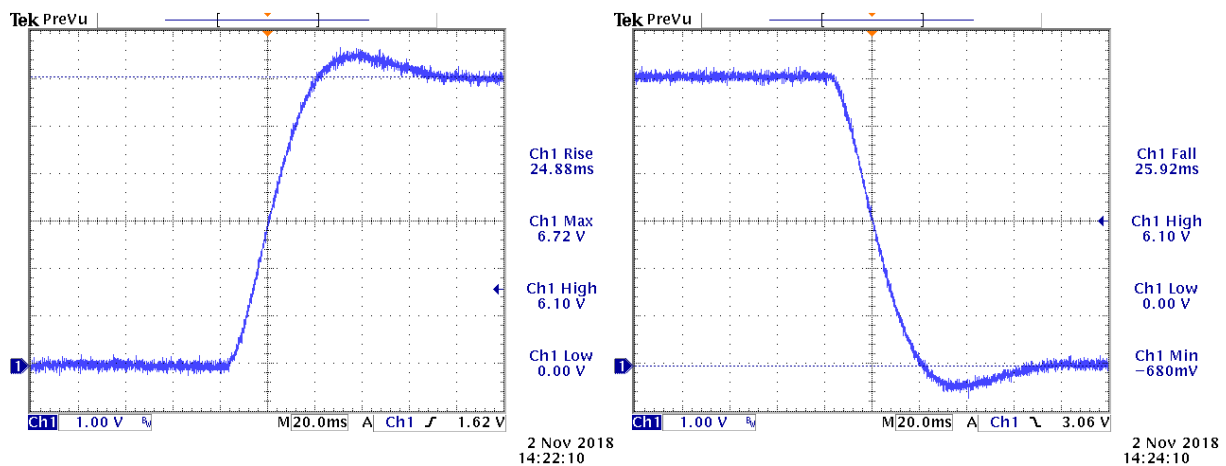


Figure 43: WAGO 750-559 analogue rise time (left) and fall time (right)

4.4.4 Connection Characterization CC and RTS in Sequential Approach

This benchmark follows the connection handling as described for case study 1 in chapter 4.3.1. As required for this case study, there are three variables read and two variables written to the IEC61850 server. The test is opening a TCP/IP connection, then writing and reading the values and closing the connection again. This sequence consists of a number of TCP/IP packages. To understand the delay induced by the whole process, in this test the CC is connected directly to the SC and in turn the SC directly to the RTS, as depicted in Figure 39. On the CC, no power allocation algorithm is running. The CC sets a static value “Val1” from Table 7 on each MMS server. When all MMS servers are written, it starts again by setting “Val2” from Table 7. This process is repeated more than 1 000 times to create a meaningful sample quantity. The time measurement is performed by the RTS. The CC sends a trigger signal to the RTS before starting to write the MMS servers. Then, the RTS starts to count the time steps while it receives the current status of all BESSs from the SC. When “Val1” is used, the counter is stopped in case it

reaches -500 as the output power. If “Val2” is used, the counter is stopped in case it reaches -51 as the output power. This measurement includes the delay induced by the communication between the SC and the RTS as described in section 4.4.2.

Number of BESS	Val 1	Val2	Simulation time step [μs]	Send interval [iterations]
1 BESS	-500	-1	50	50
5 BESS	-50	-1	50	50
50 BESS	-10	-1	50	50

Table 7: Test configurations for the sequential write test

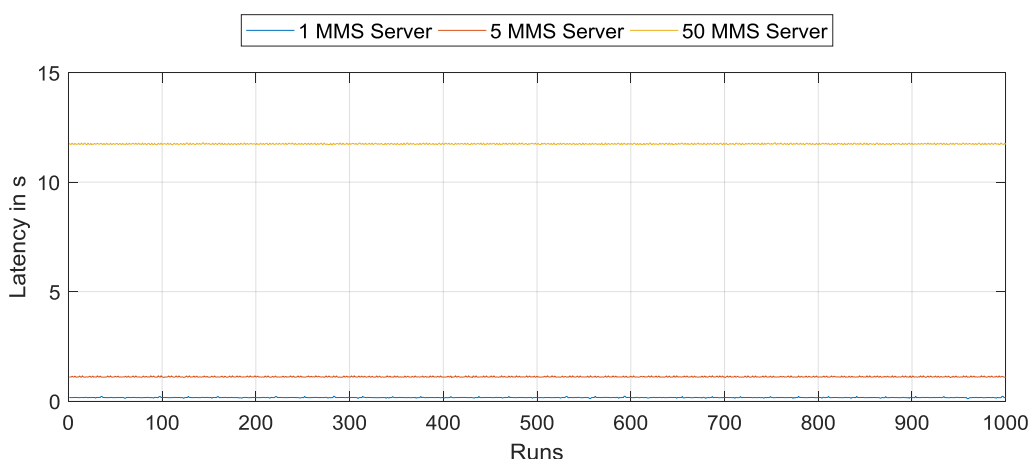


Figure 44: Communication latency between RTS and CC with sequential approach

In Table 8, the results are shown for the different configurations introduced in Table 7. The raw data for the first 1 000 runs and different configurations are shown in Figure 44. In addition to the overall delay, in the “Mean” column of Table 8, which contains the communication between the CC through the SC to the RTS, the delay between CC and SC is calculated. This calculation rests on the results as provided in section 4.4.2 and is shown as “Mean MMS”.

Configuration	Runs	Mean [s]	Mean MMS [s]	Median [s]	Max [s]	Min [s]	Standard deviation [ms]
1 BESS	1 039	0.16	--	0.16	0.22	0.11	11.91
5 BESS	1 032	1.11	1.10	1.11	1.16	1.08	20.19
50 BESS	1 028	11.75	11.74	11.73	11.80	11.70	23.50

Table 8: Statistics characterization CC to RTS communication with sequential approach

4.4.5 Connection Characterization between CC, Switch and SC in Sequential Approach

In a “real-world” setup with multiple BESSs, a switch is needed to connect the different BESSs. A switch is expected to change the behaviour of the overall system. It might induce latencies or package losses, depending on the load situation of the switch. To provide a basic understanding, latency tests with one switch (Figure 40) are conducted and compared to the results presented in section 4.4.4. The latency induced under very light load conditions is negligible, as it can be seen from the measurements in Table 9. The comparison of the delay induced when running the 5 BESS configuration with and without a switch is shown in Figure 45. It turns out that the results in Table 8 without a switch and in Table 9 with a switch are almost identical.

Configuration	Runs	Mean [s]	Median [s]	Max [s]	Min [s]	Standard deviation [ms]
1 BESS	1 133	0.16	0.16	0.22	0.11	11.70
5 BESS	1 042	1.11	1.11	1.16	1.08	20.40
50 BESS	1 039	11.75	11.74	11.80	11.71	23.40

Table 9: Statistics characterization CC to RTS communication including switch with sequential approach



Figure 45: Communication latency CC to RTS including switch, with sequential approach

4.4.6 Connection Characterization CC and SC in Parallel Approach

This benchmark follows the connection handling as described for case study 2 in chapter 4.3.2. The connection is opened for a number n of BESSs when the program on the CC is started. After the initialization step, the CC sets the analogue output to high. Then, the CC reads and writes values to all n IEC61850 servers. The output power summed up over all servers has a

value of -500 or -5 after one completed write cycle. Based on the output power, the RTS detects when the cycle is finished, in the same manner as described for the sequential connection test, compare section 4.4.4. To create a statistical meaningful sample size, this benchmark is run more than 1 000 times for each number n of BESSs.

The delay induced by the communication can be reduced by setting the cycle time in the CodeSys development environment for the IEC61850 client to a fixed number. Since this test compares different amounts of BESSs, the cycle time is set to the free run mode. This causes a waiting delay after each run of the IEC61850 client. This delay can have a significant impact, since the client is called multiple times during one interaction. The fixed cycle mode, however, is not feasible, because the minimum cycle time has to be determined for each test. Further, the development environment does not provide a way to determine this time analytically. Therefore, it needs to be tested empirically for each configuration. This is not a feasible solution since the main cycle time is influenced by task interactions, namely race conditions, which are very hard to identify. The fixed cycle time mode is analysed in more detail at the end of this section based on the one BESS configuration. It is important to state that running the software with a fixed cycle time may result in race conditions, which can be solved by increasing the cycle time.

The benchmark results are shown in Figure 46. The statistical analysis is provided in Table 10. It can be seen that the delays are significantly lower than the measurements from the sequential approach in Table 8, which is to be expected. The increase in mean delay over the number of BESSs is shown in Figure 47.

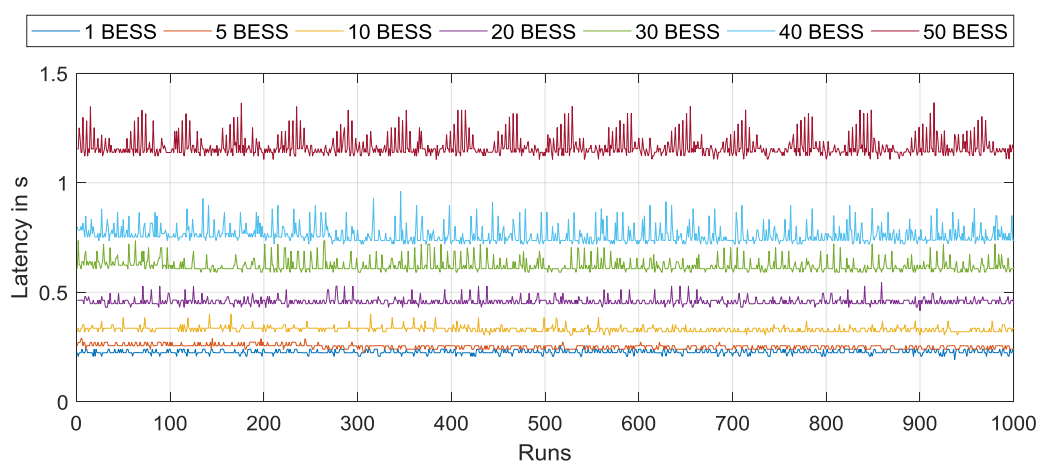


Figure 46: Communication latency CC to RTS including switch with parallel approach

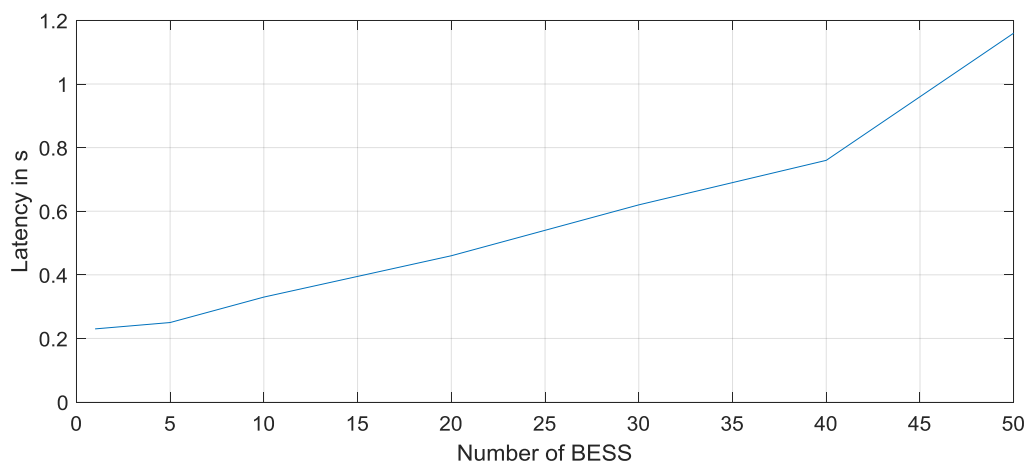


Figure 47: Increase in mean delay over the number of BESS with parallel approach

Configuration	Runs	Mean [s]	Median [s]	Max [s]	Min [s]	Standard deviation [ms]
1 BESS	1 033	0.23	0.22	0.26	0.19	9.35
5 BESS	1 080	0.25	0.26	0.29	0.22	9.87
10 BESS	1 088	0.33	0.34	0.40	0.30	12.29
20 BESS	1 031	0.46	0.45	0.54	0.41	16.01
30 BESS	1 072	0.62	0.61	0.74	0.59	28.20
40 BESS	1 024	0.76	0.75	0.96	0.72	38.93
50 BESS	1 067	1.16	1.15	1.37	1.11	46.02

Table 10: Statistics characterization CC to RTS communication including switch with parallel approach

To compare the free running mode with a fixed cycle time of 6 ms, a test with one BESS is performed. This test shows that the mean delay of 122 ms in communication with the fixed cycle time becomes nearly half of the delay in the free running mode with 230 ms. The result is provided in Table 11 and the raw data for the first 1 000 runs is shown in Figure 48. The delay difference can be explained with a 10 ms delay after each cycle in the free running mode, which is a major source of delay when the overall time needed for one cycle is low, as it is the case for one BESS.

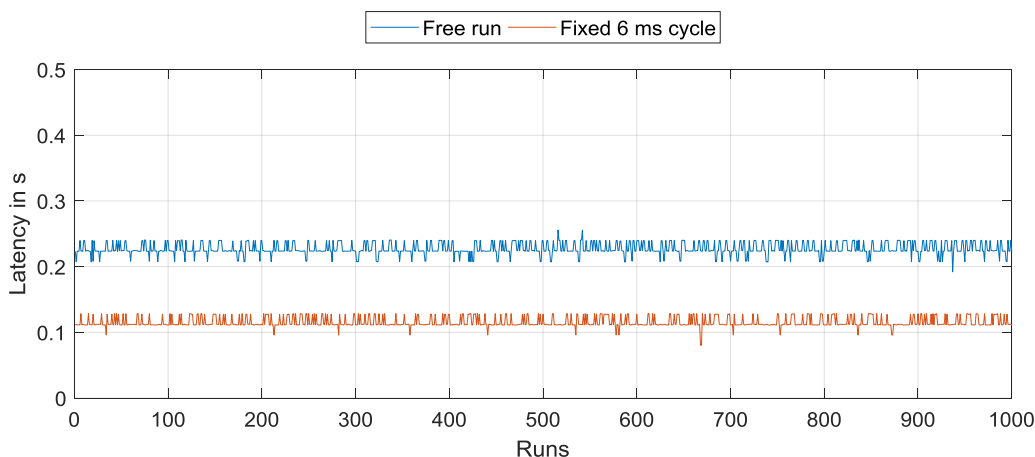


Figure 48: Communication latency CC to RTS including switch with parallel approach (fixed and free run)

Configuration	Runs	Mean [s]	Median [s]	Max [s]	Min [s]	Standard deviation [ms]
1 BESS free run	1 033	0.23	0.22	0.26	0.19	9.35
1 BESS 6 ms cycle	1 113	0.12	0.11	0.13	0.08	7.46

Table 11: Statistics characterization CC to RTS communication including switch with parallel approach (fixed and free run)

4.4.7 Performance Evaluation of the Power Allocation Algorithm

The power allocation algorithm grounds on the algorithm described in section 4.2.4. This algorithm represents the actually used power allocation algorithm. In this setup, it is possible to run the software on the CC with and without the power allocation algorithm. That way it is possible to identify the delay induced by the algorithm itself and to compare its behaviour under different numbers of BESSs. To measure the time the algorithm needs for execution, an analogue output of the CC is set to high when the algorithm is running. It is set to low again when the algorithm terminates. The duration of time the analogue output is set to low is measured with the RTS.

Since the analogue trigger time rise time is approximately 25 ms, see section 4.4.3, it is necessary to measure multiple power allocation algorithm runs on the CC. The number of power allocation algorithm runs performed for one measurement is listed in Table 12 as “Allocation Runs”. To calculate the time one run requires, the “Mean” value must be divided by the number of “Allocation Runs”. The result is provided in Table 12 in column “Time per run”. The time increases nearly linearly from 5.22 μs for one BESS to 1.99 ms for 500 BESSs.

Configura-tion	Runs	Allocation Runs	Mean [ms]	Time per Run [μs]	Median [ms]	Max [ms]	Min [ms]	Standard de- viation [ms]
1 BESS	2 030	30 000	156.5	5.22	154.4	282.3	138.2	16.3
5 BESS	2 103	6 000	126.9	21.15	122.6	250.4	106.1	12.6
10 BESS	2 122	3 000	122.4	40.8	122.5	266.5	106.1	15.1
20 BESS	2 036	1 500	120.5	80.33	122.4	250.6	91.1	13.6
50 BESS	2 087	600	118.9	198.17	122.4	250.3	106.0	12.4
500 BESS	2 067	60	119.4	1990.0	122.4	250.6	106.0	13.7

Table 12: Power allocation algorithm measured runtime

4.5 Results

4.5.1 Results Case Study 1

Case study 1 uses the sequential approach to connect to the simulated BESSs. Based on the results of the system characterization in section 4.4, the most relevant delay is the time needed for writing new values to the SC’s IEC61850 server. For this reason, it is expected that the overall test including the power allocation algorithm execution plus the communication, as depicted in Figure 31 and Figure 39, should be similar to the results of section 4.4.4.

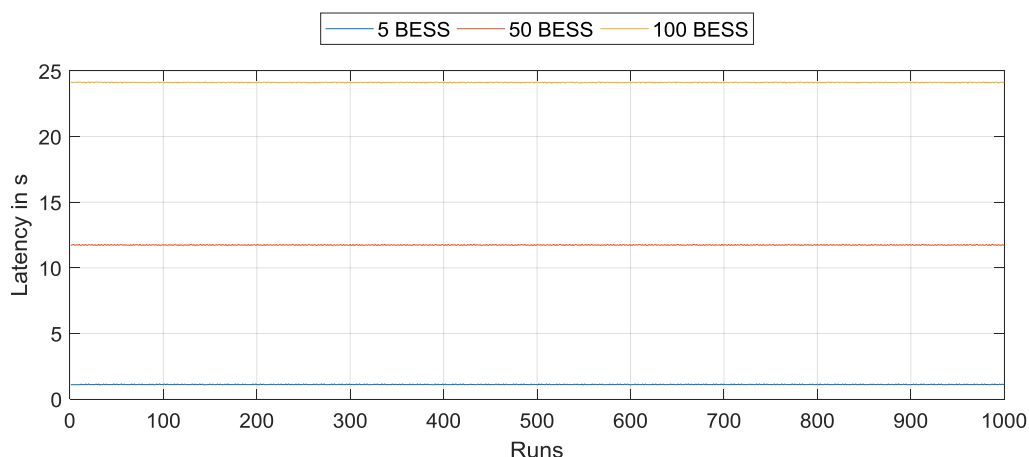


Figure 49: Communication latency full system with sequential approach

The results of the time measurements in Table 13 show that the time needed to write five BESS is 1.12 s and for 100 BESS 24.12 s. The raw data for the first 1 000 runs and different configurations is shown in Figure 49. The time needed for 100 BESSs is 21.5 times the time

required for five BESSs, which confirms the assumption of a linear relation. As predicted beforehand, the results are almost identical to the results of the communication test performed in section 4.4.4.

Configuration	Runs	Mean [s]	Median [s]	Max [s]	Min [s]	Standard deviation [ms]
5 BESS	1 155	1.12	1.11	1.17	1.08	20.50
50 BESS	1 088	11.74	11.73	11.80	11.71	23.30
100 BESS	1 307	24.12	24.13	24.17	24.06	23.78

Table 13: Statistics CC to RTS including switch latency with sequential approach

4.5.2 Results Case Study 2

Case study 2 uses the parallel approach to connect to the simulated BESSs. Based on the results of the system characterization in chapter 4.4, the most relevant delay is the time required for writing new values to the SC’s IEC61850 server. Thus, it is expected that the overall test including the power allocation algorithm execution and communication as depicted in Figure 50 should be similar to the results of the parallel connection setup between RTS and CC in section 4.4.5.

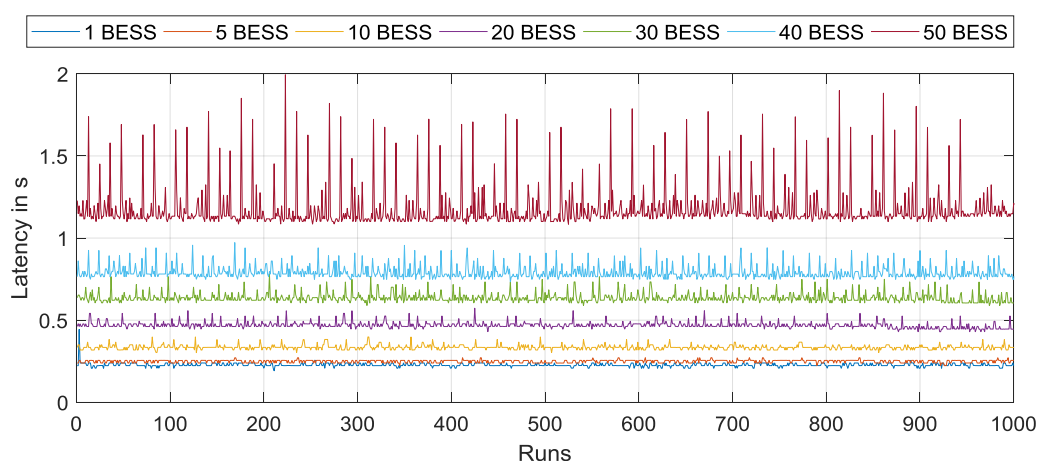


Figure 50: Communication latency full system with parallel approach

The results of the time measurements show that the time needed to write five BESSs is 25 ms and for 50 BESSs 1.18 s. The time needed for 50 BESSs is about 4.7 times the time required for five BESSs. As predicted, the results are almost identical with the results for the communication test performed in section 4.4.5. The full statistics of the test are shown in Table 14.

Configuration	Runs	Mean [s]	Median [s]	Max [s]	Min [s]	Standard deviation [ms]
1 BESS	1 058	0.23	0.22	0.44	0.19	11.46
5 BESS	1 221	0.25	0.26	0.27	0.22	8.46
10 BESS	1 093	0.33	0.33	0.40	0.30	13.68
20 BESS	1 132	0.47	0.46	0.57	0.43	19.51
30 BESS	1 105	0.63	0.62	0.78	0.59	29.48
40 BESS	1 099	0.79	0.78	0.99	0.73	40.03
50 BESS	1 117	1.18	1.13	1.99	1.08	127.09

Table 14: Statistics of full system test with parallel approach

4.6 Conclusion

Based upon the overall HiL setup, it has been shown in the previous sections that when setting a new power set-point to different ELSA BESSs in parallel, the total time delay – from setting a new power demand set-point until the set-point arrives at the RTS – is 23 ms. For 50 BESSs, this time delay increases to 1.18 s. The approach is limited to 50 BESSs for memory limitation reasons in the DUT. In this context, it should be stated that one BESS in the DT5 system represents 96 kW of peak power and 12 kWh of energy stored. This would result in 9.6 MW of output power and 1.2 MWh of available energy for 100 BESSs. When a sequential approach is selected, the time required for setting five BESS is 1.12 s and for 100 BESSs 24.12 s. The sequential approach is slower than the parallel approach and the time required for setting the new power set-points increases linearly with the number of BESSs installed. On the opposite, the sequential approach can support a significantly larger number of BESSs. Although at most a number of 50 BESSs were successfully tested in the parallel case, this does not mean that this is the upper technical limit for the BESS aggregation purpose.

5 Conclusions and Lessons Learned

This deliverable provides the impact analysis for scenarios covering different use cases for large-scale ELSA BESS applications as well as the technical analysis of the ELSA BESS communication infrastructure. Based on the fact that field trials are always limited in size, far larger scenarios compared to field trial possibilities are evaluated by upscaling the ELSA BESS in simulation taking into consideration crucial ICT aspects. The different scenarios for the upscaled simulation are defined and implemented in appropriate simulation tools. Modelling of components is performed representing the level of detail that is required for the analyses.

As the major finding of this work, it turns out that the ELSA system is scalable to a certain extent. More precisely, it can be concluded that at least 50 ELSA BESSs can be aggregated and controlled, so that additional use cases become both feasible and economically viable. Examples are primary control reserve or the participation to the national energy trade market. It is demonstrated that for such large-scale use cases at least 15 – 20 ELSA BESSs are required to satisfy the physical and regulatory battery storage power and capacity requirements.

For the technical validation of the BESS aggregation concept, a HiL approach is chosen to investigate and to understand the latency behaviour of the communication between a coordinated controller unit and the different ELSA BESSs, since the costs for upscaling the physical ELSA system would exceed the available project funding. Using this HiL setup, multifarious scalability tests are performed with the objective to evaluate the limits of the ELSA BESS communication infrastructure. From the scalability tests, it can be stated that the control of 50 ELSA BESSs can be either done in a sequential or in parallel way. The control of up to 100 BESSs was proven feasible with the sequential approach. For the sequential approach, a communication connection is established, data is read or written and the connection is closed again for each of the ELSA BESSs consecutively. The main advantage of this sequential approach is in the large number of ELSA BESSs that can be controlled by the same hardware, whereas the disadvantage is in the linear increase of time needed to update all the ELSA BESSs sequentially. Instead, the parallel approach connects to all BESSs simultaneously and leaves the connections open. This approach is faster in controlling the ELSA BESSs in comparison to the sequential approach, but requires more program memory in the controller unit and is therefore limited to at most 50 ELSA BESSs with the hardware used during this work.

Because of time planning issues, an example software for the DUT was developed at RWTH Aachen University and a DUT was purchased. The purchased DUT is a slightly different version compared to the real control hardware used in the ELSA DT5 system. Nevertheless, the development of the DUT software was done as close as possible to the real system, which was not available at that point in time. It was ensured that all the involved partners were in close contact for the power allocation algorithm development as well as for the definition of interchanged variables via IEC61850. We see no problems in exchanging the DUT developed at

RWTH Aachen University and the DUT developed by Renault, Nissan and Bouygues, since the used protocol standard (IEC61850) is the same and the hardware is basically identical except for different licenses installed. The results obtained with our version of the DUT are expected to be very similar compared to the real control hardware of the ELSA DT5 system.

As lessons learned mainly the delays in the delivery of the real DUT should be named. Fortunately, this was mostly compensated by developing a simplified DUT at RWTH Aachen University. In general, the communication within joint research projects is always a challenge and can be improved. This applies especially to an intercultural environment, but the challenges are always outweighed by the benefit of different backgrounds (science, industry and others) as well as the resulting variety of new ideas and improvements.

References

- [1] Energy Local Storage Advanced system (ELSA), *Deliverable 6.3: Results of service evaluation*.
- [2] Energy Local Storage Advanced system (ELSA), *Deliverable 6.1: Design optimization environment*.
- [3] M. Diekerhof, S. Schwarz, and A. Monti, "Multiobjective Optimization for Demand Response Services from a Battery Storage System (Accepted - not published yet)," in *2018 IEEE PES ISGT Europe*, pp. 1–6.
- [4] RTDS Technologies Inc., *RSCAD® - POWER SYSTEM SIMULATION SOFTWARE*. [Online] Available: <https://www.rtds.com/the-simulator/our-software/about-rscad/>. Accessed on: Nov. 08 2018.
- [5] RTDS Technologies Inc., *Real Time Digital Power System Simulator: RTDS® Simulator*. [Online] Available: <https://www.rtds.com/>. Accessed on: Nov. 08 2018.
- [6] M. Chen and G. A. Rincon-Mora, "Accurate Electrical Battery Model Capable of Predicting Runtime and I–V Performance," *IEEE Transactions on Energy Conversion*, vol. 21, no. 2, pp. 504–511, 2006.
- [7] J. Rodriguez, S. Bernet, P. K. Steimer, and I. E. Lizama, "A Survey on Neutral-Point-Clamped Inverters," *IEEE Transactions on Industrial Electronics*, vol. 57, no. 7, pp. 2219–2230, 2010.
- [8] N. Celanovic and D. Boroyevich, "A comprehensive study of neutral-point voltage balancing problem in three-level neutral-point-clamped voltage source PWM inverters," *IEEE Transactions on Power Electronics*, vol. 15, no. 2, pp. 242–249, 2000.
- [9] U.-M. Choi, J.-S. Lee, and K.-B. Lee, "New Modulation Strategy to Balance the Neutral-Point Voltage for Three-Level Neutral-Clamped Inverter Systems," *IEEE Transactions on Energy Conversion*, vol. 29, no. 1, pp. 91–100, 2014.
- [10] A. Bendre, G. Venkataramanan, D. Rosene, and V. Srinivasan, "Modeling and design of a neutral-point voltage regulator for a three-level diode-clamped inverter using multiple-carrier modulation," *IEEE Transactions on Industrial Electronics*, vol. 53, no. 3, pp. 718–726, 2006.
- [11] C. Newton and M. Sumner, "Neutral point control for multi-level inverters: theory, design and operational limitations," in *IAS '97. Conference Record of the 1997 IEEE Industry Applications Conference Thirty-Second IAS Annual Meeting, New Orleans, LA, USA, Oct. 1997*, pp. 1336–1343.

-
- [12] Allgäuer Überlandwerk GmbH, *Aus Liebe zum Allgäu*. [Online] Available: <https://www.auew.de/>. Accessed on: Nov. 06 2018.
- [13] German Federal Ministry of Justice and Consumer Protection, *Gesetz für den Ausbau erneuerbarer Energien (Erneuerbare-Energien-Gesetz - EEG 2017)*. [Online] Available: http://www.gesetze-im-internet.de/eeg_2014/EEG_2017.pdf. Accessed on: Nov. 06 2018.
- [14] EPEX SPOT SE, *Welcome*. [Online] Available: <https://www.epexspot.com/en/>. Accessed on: Nov. 06 2018.
- [15] EPEX SPOT SE, *Day-Ahead Auction*. [Online] Available: <https://www.epexspot.com/en/market-data/dayaheadauction>. Accessed on: Nov. 06 2018.
- [16] EPEX SPOT SE, *Intraday Auction*. [Online] Available: <https://www.epexspot.com/en/market-data/intradayauction>. Accessed on: Nov. 06 2018.
- [17] EPEX SPOT SE, *Intraday Continuous*. [Online] Available: <https://www.epexspot.com/en/market-data/intradaycontinuous>. Accessed on: Nov. 06 2018.
- [18] German Bundesnetzagentur and German Bundeskartellamt, *Monitoringbericht 2017: Monitoringbericht gemäß § 63 Abs. 3 i. V. m. § 35 EnWG und § 48 Abs. 3 i. V. m. § 53 Abs. 3 GWB*. [Online] Available: https://www.bundesnetzagentur.de/SharedDocs/Downloads/DE/Allgemeines/Bundesnetzagentur/Publikationen/Berichte/2017/Monitoringbericht_2017.pdf. Accessed on: Nov. 06 2018.
- [19] Allgäuer Überlandwerk GmbH, *Grundversorgung (Allgemeiner Tarif)*. [Online] Available: <https://www.auew.de/grundversorgung-2/>. Accessed on: Nov. 06 2018.
- [20] German Bundesnetzagentur, *EEG register data and reference values for payment*. [Online] Available: https://www.bundesnetzagentur.de/EN/Areas/Energy/Companies/RenewableEnergy/Facts_Figures_EEG/Register_data_tariffs/EEG_registerdata_payments_node.html. Accessed on: Nov. 06 2018.
- [21] N. Wirtz and A. Monti, "Battery Storage Utilization For Cost and Imbalance Reduction In A Balancing Group (Accepted - not published yet)," in *2018 IEEE PES ISGT Europe*, pp. 1–6.
- [22] European Network of Transmission System Operators for Electricity (ENTSO-E), *Home*. [Online] Available: <https://www.entsoe.eu/>. Accessed on: Nov. 08 2018.
- [23] Regelleistung Online GbR, *General information on control reserve - technical aspects*. [Online] Available: <https://www.regelleistung.net/ext/static/technical?lang=en>. Accessed on: Nov. 06 2018.
-

- [24] Regelleistung Online GbR, *Eckpunkte und Freiheitsgrade bei Erbringung von Primärregel-leistung: Leitfaden für Anbieter von Primärregelleistung*. [Online] Available: <https://www.regelleistung.net/ext/download/eckpunktePRL>. Accessed on: Nov. 08 2018.
- [25] Regelleistung Online GbR, *Prognose: Deutlicher Rückgang der PRL Erlöse in 2018 | Regel-leistung-Online*. [Online] Available: <https://www.regelleistung-online.de/prl-prognose-2018/>. Accessed on: Nov. 09 2018.
- [26] J. Fler *et al.*, “Model-based Economic Assessment of Stationary Battery Systems Provid-ing Primary Control Reserve,” *Energy Procedia*, vol. 99, pp. 11–24, 2016.
- [27] International Electrotechnical Commission (IEC), *IEC61850: Communication networks and systems for power utility automation*.
- [28] MZ Automation GmbH and GitHub Inc., *Official repository for libIEC61850, the open-source library for the IEC 61850 protocols*. [Online] Available: <https://github.com/mz-au-tomation/libiec61850>. Accessed on: Nov. 09 2018.
- [29] Daniel Veillard, *libxml2: The XML C parser and toolkit of Gnome*. [Online] Available: <http://xmlsoft.org/>. Accessed on: Nov. 09 2018.
- [30] Institute for Automation of Complex Power Systems, EON.ERC, and RWTH Aachen Uni-versity, *VILLASweb*. [Online] Available: <http://fein-aachen.org/projects/villas-web/>. Ac-cessed on: Nov. 09 2018.
- [31] X. LI, L. YAO, and D. HUI, “Optimal control and management of a large-scale battery en-ergy storage system to mitigate fluctuation and intermittence of renewable generations,” *Journal of Modern Power Systems and Clean Energy*, vol. 4, no. 4, pp. 593–603, 2016.
- [32] WAGO Kontakttechnik GmbH & Co. KG, *Ihr Partner für Automatisierungs- und Verbin-dungstechnik*. [Online] Available: <https://www.wago.com/de/>. Accessed on: Nov. 08 2018.
- [33] WAGO Kontakttechnik GmbH & Co. KG, *WAGO 4-Kanal-Analogausgang 750-559: DC 0 ... 10 V*. [Online] Available: <https://www.wago.com/de/io-systeme/4-kanal-analo-gausgang/p/750-559>. Accessed on: Nov. 08 2018.
- [34] CODESYS Group, *CODESYS Development System: The IEC 61131-3 Programming Tool for the Industrial Controller and Automation Technology Sector*. [Online] Available: <https://www.codesys.com/products/codesys-engineering/development-system.html>. Accessed on: Nov. 08 2018.

-
- [35] WAGO Kontakttechnik GmbH & Co. KG, *Manual 759-911 - Version 1.7.0: IEC 61850 Solution for programmable Controls of Telecontrol Technology*. [Online] Available: <https://www.wago.com/>. Accessed on: Nov. 09 2018.
- [36] Hewlett Packard Enterprise Development LP, *HP ProCurve 1800-24G*. [Online] Available: <https://www.hpe.com/>. Accessed on: Nov. 08 2018.
- [37] Dell Inc., *PowerEdge R440 Rack Server*. [Online] Available: <https://www.dell.com/en-en/work/shop/productdetailstxn/poweredge-r440>. Accessed on: Nov. 08 2018.
- [38] Intel Corporation, *Intel® Xeon® Silver 4114 Processor: 13.75M Cache, 2.20 GHz*. [Online] Available: <https://ark.intel.com/products/123550/Intel-Xeon-Silver-4114-Processor-13-75M-Cache-2-20-GHz->. Accessed on: Nov. 08 2018.
- [39] Intel Corporation, *Intel® Ethernet-Converged-Network-Adapter X710-T4*. [Online] Available: <https://ark.intel.com/de/products/93428/Intel-Ethernet-Converged-Network-Adapter-X710-T4>. Accessed on: Nov. 08 2018.
- [40] WAGO Kontakttechnik GmbH & Co. KG, *WAGO Controller PFC200 750-8206: 2 x ETHERNET, RS-232/-485, CAN, CANopen, PROFIBUS Slave*. [Online] Available: <https://www.wago.com/gb/plcs-controllers/controller-pfc200/p/750-8206>. Accessed on: Nov. 08 2018.
- [41] Gurobi Optimization Inc., *Gurobi Optimizer*. [Online] Available: <http://www.gurobi.com/>. Accessed on: Nov. 08 2018.
- [42] J. Leithon, T. J. Lim, and S. Sun, "Battery-Aided Demand Response Strategy Under Continuous-Time Block Pricing," *IEEE Transactions on Signal Processing*, vol. 64, no. 2, pp. 395–405, 2016.
- [43] M. Gonzalez Vaya, G. Andersson, and S. Boyd, "Decentralized control of plug-in electric vehicles under driving uncertainty," in *IEEE PES Innovative Smart Grid Technologies, Europe*, Istanbul, Turkey, Oct. 2014 - Oct. 2014, pp. 1–6.

ANNEX A: Mathematical Optimization Model for the Large-scale BESS Use Case Simulations

The mathematical optimization model for the large-scale BESS use case simulations is defined by the set of physical constraints in equations (A.1) – (A.18), compare section 2.3.1 as well as Figure 3. These constraints are implemented using the Python programming language and the Gurobi mathematical programming solver [41]. It is important to mention that the relationship among the different optimization variables in (A.1) – (A.18) is inspired by the work of Leithon et al. in [42].

$$P_{El\text{discharge}_{min}} \leq P_{El\text{Batt}_{discharge}_t} \leq P_{El\text{discharge}_{max}}, \quad \forall t \in T \quad (\text{A.1})$$

$$P_{El\text{charge}_{min}} \leq P_{El\text{Batt}_{charge}_t} \leq P_{El\text{charge}_{max}}, \quad \forall t \in T \quad (\text{A.2})$$

$$P_{El\text{Batt}_t} = P_{El\text{Batt}_{charge}_t} \cdot T_{charge}_t + P_{El\text{Batt}_{discharge}_t} \cdot T_{discharge}_t, \quad \forall t \in T \quad (\text{A.3})$$

$$\hat{P}_{El\text{Batt}_t} = P_{El\text{Batt}_{charge}_t} \cdot \eta_{charge} \cdot T_{charge}_t + \frac{P_{El\text{Batt}_{discharge}_t}}{\eta_{discharge}} \cdot T_{discharge}_t, \quad \forall t \in T \quad (\text{A.4})$$

$$T_{discharge}_t + T_{charge}_t \leq 1, \quad \forall t \in T \quad (\text{A.5})$$

$$T_{discharge}_t \in \{0,1\}, \quad \forall t \in T \quad (\text{A.6})$$

$$T_{charge}_t \in \{0,1\}, \quad \forall t \in T \quad (\text{A.7})$$

$$E_{\text{Batt}_t} = E_{\text{Batt}_{t-1}} + \hat{P}_{El\text{Batt}_t} \cdot \Delta t, \quad \forall t \in T \quad (\text{A.8})$$

$$E_{\text{Batt}_{t=-1}} = SoC_{ini} \cdot E_{\text{Batt}_{max}}, \quad \forall t \in T \quad (\text{A.9})$$

$$E_{\text{Batt}_{t=T}} = E_{\text{Batt}_{t=-1}}, \quad \forall t \in T \quad (\text{A.10})$$

$$0 \leq E_{\text{Batt}_t} \leq E_{\text{Batt}_{max}}, \quad \forall t \in T \quad (\text{A.11})$$

$$0 \leq P_{ElG_t} \leq P_{ElG_{max}}, \quad \forall t \in T \quad (\text{A.12})$$

$$0 \leq P_{ElU_t} \leq P_{ElU_{max}}, \quad \forall t \in T \quad (\text{A.13})$$

$$P_{ElGrid_t} = P_{ElG_t} \cdot T_{G_t} + P_{ElU_t} \cdot T_{U_t}, \quad \forall t \in T \quad (\text{A.14})$$

$$T_{G_t} + T_{U_t} \leq 1, \quad \forall t \in T \quad (\text{A.15})$$

$$T_{G_t} \in \{0,1\}, \quad \forall t \in T \quad (\text{A.16})$$

$$T_{U_t} \in \{0,1\}, \quad \forall t \in T \quad (\text{A.17})$$

$$0 = P_{ElPV_t} - P_{ElDemand_t} + P_{ElBatt_t} + P_{ElGrid_t}, \quad \forall t \in T \quad (\text{A.18})$$

In the general case, the optimization is carried out over a specific simulation horizon T , for instance day-ahead, with $t \in T$ timesteps. Both (A.1) and (A.2) represent the physical limitations of the large-scale BESS for the lower and upper charging/discharging limits. Equation (A.3) describes the net electrical power flow of the BESS during time step t . Additionally, equation (A.4) includes the charging and discharging efficiencies η_{charge} and $\eta_{discharge}$ of the BESS. Two binary variables T_{charge_t} and $T_{discharge_t}$ that are bounded by (A.5) – (A.7) emphasize that the BESS can either charge or discharge during each time step t . Thus, the electrical power of the battery storage in one time step is either positive (charging) or negative (discharging). The electrical energy storage within the BESS is described through equations (A.8) – (A.11). The current SoC, i.e., the energy stored in time step t , is described through equation (A.8) and is closely linked to the expression in (A.11) describing the physical storage limitations. The duration of one time step t is denoted with Δt . Further, the expressions in (A.9) and (A.10) force the SoC at the end of the optimization horizon to be equal to the initial SoC. This is similar to the work in [43] in order to avoid myopic storage behaviour. Otherwise and under certain circumstances, the optimization might shift all the expensive purchase beyond the optimization horizon. The overall power exchange with the electrical network, i.e., with the electrical grid during time step t , is described through equation (A.14) and is characterized by the variable P_{ElGrid_t} . This variable contains the electrical power provided to the (network) utility P_{ElU_t} defined in (A.13) and the received power from the network P_{ElG_t} defined in (A.12). The formulation in (A.15) causes the electrical power not to flow to and from the grid at the same time, due to the two binary variables T_{G_t} and T_{U_t} defined in (A.16) and

(A.17). Thus, in the case where power is received from the grid in time step t , P_{ElGrid_t} is negative, whereby, e.g., the feed-in of PV generation or battery discharging power during time step t cause a positive value of P_{ElGrid_t} . Finally, expression (A.18) ensures the total electrical power balance at the PCC for the entire optimization horizon T .

ANNEX B: Participation to the National Energy Trade Market Use Case – Mathematical Optimization Problem Formulation

The mathematical optimization problem formulation defined by equations (B.1) – (B.21) with the objective function in equation (B.1) and with the constraints besides (A.1) – (A.18) in (B.2) – (B.21) are provided below. The optimization is embedded into a MPC rolling horizon framework, see section 3.3.1. Moreover, the formula symbols used in equations (B.1) – (B.21), and as not explained in sections 2.3.1 and 3.3 beforehand, are provided subsequently.

$$\min \sum_{\tau \in \mathcal{T}} \Delta\tau \cdot \left[-P_{El_{PV.District\tau}} \cdot C_{PV.District} - P_{El_{PV.EEG\tau}} \cdot C_{PV.EEG} - P_{El_{Batt.PV.District\tau}} \cdot C_{PV.District} - P_{El_{Batt.PV.EEG\tau}} \cdot C_{PV.EEG} + P_{El_{A.District\tau}} \cdot C_{A\tau} + P_{El_{B.District\tau}} \cdot C_{B\tau} + P_{El_{C.District\tau}} \cdot C_{C\tau} + P_{El_{A.Batt\tau}} \cdot C_{A\tau} + P_{El_{B.Batt\tau}} \cdot C_{B\tau} + P_{El_{C.Batt\tau}} \cdot C_{C\tau} + P_{El_{Grid.District\tau}} \cdot C_{Grid} + P_{El_{Grid.Batt\tau}} \cdot C_{Grid} \right] \quad (B.1)$$

$$P_{El_{PV\tau}} = P_{El_{PV.District\tau}} + P_{El_{PV.Batt\tau}} + P_{El_{PV.EEG\tau}}, \quad \forall \tau \in \mathcal{T} \quad (B.2)$$

$$0 = P_{El_{PV.District\tau}} + P_{El_{Batt.PV.District\tau}} \cdot T_{Batt.PV.Discharge\tau} + P_{El_{Batt.Market.District\tau}} \cdot T_{Batt.Market.Discharge\tau} + P_{El_{Batt.Grid.District\tau}} \cdot T_{Batt.Grid.Discharge\tau} - P_{El_{District.Demand\tau}} + P_{El_{Market.District\tau}} + P_{El_{Grid.District\tau}}, \quad \forall \tau \in \mathcal{T} \quad (B.3)$$

$$T_{Batt.PV.Charge\tau} + T_{Batt.PV.Discharge\tau} \leq 1, \quad \forall \tau \in \mathcal{T} \quad (B.4)$$

$$T_{Batt.Grid.Charge\tau} + T_{Batt.Grid.Discharge\tau} \leq 1, \quad \forall \tau \in \mathcal{T} \quad (B.5)$$

$$T_{Market.Batt.Charge\tau} + T_{Market.Batt.Discharge\tau} \leq 1, \quad \forall \tau \in \mathcal{T} \quad (B.6)$$

$$T_{Batt.PV.Charge\tau}, T_{Batt.PV.Discharge\tau}, T_{Batt.Grid.Charge\tau}, T_{Batt.Grid.Discharge\tau}, T_{Market.Batt.Charge\tau}, T_{Market.Batt.Discharge\tau} \in \{0,1\}, \quad \forall \tau \in \mathcal{T} \quad (B.7)$$

$$E_{El_{A.Blocked\tau}} = P_{El_{A.Blocked\tau}}^* \cdot \Delta\tau, \quad \forall \tau \in \mathcal{T} \quad (B.8)$$

$$E_{El_{A.Blocked\tau}} = P_{El_{A.Blocked\tau}}^* \cdot \Delta\tau, \quad \forall \tau \in \mathcal{T} \quad (B.9)$$

$$P_{El_{A.District\tau}} + P_{El_{A.Batt\tau}} = P_{El_{A.Blocked\tau}}^*, \quad \forall \tau \in \mathcal{T} \quad (B.10)$$

$$P_{ElB.District\tau} + P_{ElB.Batt\tau} = P_{ElB.Blocked\tau}^*, \quad \forall \tau \in \mathcal{T} \quad (B.11)$$

$$P_{ElC.District\tau} + P_{ElC.Batt\tau} = P_{ElC.Blocked\tau}^* + P_{ElC.Blocked\tau}, \quad \forall \tau \in \mathcal{T} \quad (B.12)$$

$$P_{ElA.District\tau} \geq 0, \quad P_{ElB.District\tau} \geq 0, \quad P_{ElC.District\tau} \geq 0, \quad \forall \tau \in \mathcal{T} \quad (B.13)$$

$$P_{ElMarket.District\tau} = P_{ElA.District\tau} + P_{ElB.District\tau} + P_{ElC.District\tau}, \quad \forall \tau \in \mathcal{T} \quad (B.14)$$

$$P_{ElMarket.Batt\tau} = P_{ElA.Batt\tau} + P_{ElB.Batt\tau} + P_{ElC.Batt\tau}, \quad \forall \tau \in \mathcal{T} \quad (B.15)$$

$$\begin{aligned} P_{ElBatt\tau} = & P_{ElMarket.Batt\tau} + P_{ElPV.Batt\tau} \cdot T_{Batt.PV.Charge\tau} - P_{ElBatt.PV.EEG\tau} \\ & \cdot T_{Batt.PV.Discharge\tau} - P_{ElBatt.PV.District\tau} \cdot T_{Batt.PV.Discharge\tau} \\ & + P_{ElGrid.Batt\tau} \cdot T_{Batt.Grid.Charge\tau} - P_{ElBatt.Grid.District\tau} \\ & \cdot T_{Batt.Grid.Discharge\tau}, \quad \forall \tau \in \mathcal{T} \end{aligned} \quad (B.16)$$

$$\begin{aligned} P_{ElMarket.Batt\tau} = & P_{ElMarket.Batt.Charge\tau} \cdot T_{Market.Batt.Charge\tau} - P_{ElMarket.Batt.Discharge\tau} \\ & \cdot T_{Market.Batt.Discharge\tau}, \quad \forall \tau \in \mathcal{T} \end{aligned} \quad (B.17)$$

$$P_{ElC.Blocked\tau} = 0, \quad \forall \tau \in \mathcal{T}, \tau \neq t + 2 \quad (B.18)$$

$$\begin{aligned} & P_{ElBatt.PV.EEG\tau} \cdot T_{Batt.PV.Discharge\tau} + P_{ElBatt.PV.District\tau} \cdot T_{Batt.PV.Discharge\tau} \\ & \leq \sum_{i=0}^t \left(P_{ElPV.Batt_i}^* \cdot T_{Batt.PV.Charge_i}^* - P_{ElBatt.PV.EEG_i}^* \right. \\ & \quad \left. \cdot T_{Batt.PV.Discharge_i}^* - P_{ElBatt.PV.District_i}^* \cdot T_{Batt.PV.Discharge_i}^* \right) \\ & + \sum_{i=t}^{\tau-1} \left(P_{ElPV.Batt_i} \cdot T_{Batt.PV.Charge_i} - P_{ElBatt.PV.EEG\tau} \right. \\ & \quad \left. \cdot T_{Batt.PV.Discharge\tau} - P_{ElBatt.PV.District\tau} \cdot T_{Batt.PV.Discharge\tau} \right), \\ & \forall \tau \in \mathcal{T} \end{aligned} \quad (B.19)$$

$$\begin{aligned} & P_{ElBatt.Market.District\tau} \cdot T_{Batt.Market.Discharge\tau} \\ & \leq \sum_{i=0}^t \left(P_{ElMarket.Batt_i}^* \right) + \sum_{i=t}^{\tau-1} \left(P_{ElMarket.Batt_i} \right), \quad \forall \tau \in \mathcal{T} \end{aligned} \quad (B.20)$$

$$\begin{aligned}
& P_{El_{Batt.Grid.District\tau}} \cdot T_{Batt.Grid.Discharge\tau} \\
& \leq \sum_{i=0}^{\tau} \left(P_{El_{Grid.Batt_i}}^* \cdot T_{Batt.Grid.Charge_i}^* - P_{El_{Batt.Grid.District_i}}^* \right. \\
& \quad \left. \cdot T_{Batt.Grid.Discharge_i}^* \right) \\
& + \sum_{i=t}^{\tau-1} \left(P_{El_{Grid.Batt_i}} \cdot T_{Batt.Grid.Charge_i} - P_{El_{Batt.Grid.District_i}} \right. \\
& \quad \left. \cdot T_{Batt.Grid.Discharge_i} \right), \quad \forall \tau \in \mathcal{T}
\end{aligned} \tag{B.21}$$

- $P_{El_{District.Demand\tau}}$: Total power demand of the district in time step τ
- $P_{El_{PV\tau}}$: Total PV power generation in time step τ
- $P_{El_{PV.District\tau}}$: PV power generation directly consumed by the district in time step τ
- $P_{El_{PV.Batt\tau}}$: PV power generation stored by the ELSA storage in time step τ
- $P_{El_{PV.EEG\tau}}$: PV power generation directly sold to the EEG in time step τ
- $P_{El_{Grid.District\tau}}$: Power bought from the district's local energy supplier and consumed by the district in time step τ
- $P_{El_{Grid.Batt\tau}}$: Power bought from the district's local energy supplier and stored by the ELSA storage in time step τ
- $P_{El_{Market.District\tau}}$: Power directly bought on the energy trade market by the district operator and consumed by the district in time step τ
- $P_{El_{Market.Batt\tau}}$: Power stored by the ELSA storage and traded on the energy trade market by the district operator in time step τ
- $P_{El_{Market.Batt.Charge\tau}}$: Power directly bought on the energy trade market by the district operator and stored by the ELSA storage in time step τ
- $P_{El_{Market.Batt.Discharge\tau}}$: Power stored by the ELSA storage and sold to the energy trade market by the district operator in time step τ
- $P_{El_{Batt.PV.District\tau}}$: ELSA storage discharging power consumed by the district in time step τ , which was supplied by the PV installation during earlier time steps
- $P_{El_{Batt.PV.EEG\tau}}$: ELSA storage discharging power sold to the EEG in time step τ , which was supplied by the PV installation during earlier time steps

- $P_{El_{Batt.Market.District\tau}}$: ELSA storage discharging power consumed by the district in time step τ , which was bought on the energy trade market by the district operator during earlier time steps
- $P_{El_{Batt.Grid.District\tau}}$: ELSA storage discharging power consumed by the district in time step τ , which was bought from the district's local energy supplier during earlier time steps
- $P_{El_{A.Blocked\tau}}^*$: Amount of power to receive from or to deliver to energy trade market product A in time step τ as the outcome of the first optimization stage
- $P_{El_{B.Blocked\tau}}^*$: Amount of power to receive from or to deliver to energy trade market product B in time step τ as the outcome of the first optimization stage
- $P_{El_{C.Blocked\tau}}^*$: Amount of power to receive from or to deliver to energy trade market product C in time step τ as the outcome of the second optimization stage
- $P_{El_{C.Blocked\tau}}$: Desired amount of power to receive from or to deliver to energy trade market product C in time step τ in order to maximize the district operator's profit
- $P_{El_{A.District\tau}}$: Power directly bought on the energy trade market from product A by the district operator and consumed by the district in time step τ
- $P_{El_{B.District\tau}}$: Power directly bought on the energy trade market from product B by the district operator and consumed by the district in time step τ
- $P_{El_{C.District\tau}}$: Power directly bought on the energy trade market from product C by the district operator and consumed by the district in time step τ
- $P_{El_{A.Batt\tau}}$: Power stored by the ELSA storage and traded on the energy trade market as product A by the district operator in time step τ
- $P_{El_{B.Batt\tau}}$: Power stored by the ELSA storage and traded on the energy trade market as product B by the district operator in time step τ
- $P_{El_{C.Batt\tau}}$: Power stored by the ELSA storage and traded on the energy trade market as product C by the district operator in time step τ
- $T_{Batt.PV.Charge\tau}$: Binary decision variable, if the ELSA storage should charge PV power in time step τ
- $T_{Batt.PV.Discharge\tau}$: Binary decision variable, if the ELSA storage should discharge PV power in time step τ
- $T_{Batt.Grid.Charge\tau}$: Binary decision variable, if the ELSA storage should charge power from the district's local energy supplier in time step τ

- $T_{Batt.Grid.Discharge_\tau}$: Binary decision variable, if the ELSA storage should discharge power to the district's local energy supplier in time step τ
- $T_{Market.Batt.Charge_\tau}$: Binary decision variable, if the ELSA storage should charge power from the energy trade market in time step τ
- $T_{Market.Batt.Discharge_\tau}$: Binary decision variable, if the ELSA storage should discharge power to the energy trade market in time step τ
- $C_{PV.District}$: Profit of the district operator for selling the local PV power to the district
- $C_{PV.EEG}$: Profit of the district operator for selling the local PV power to the EEG
- C_{Grid} : Costs of the district operator for supplying the district with power from the district's local energy supplier
- C_{A_τ} : Energy block price for product A in time step τ
- C_{B_τ} : Energy block price for product B in time step τ
- C_{C_τ} : Energy block price for product C in time step τ
- $\Delta\tau$: Discrete time slot duration
- $P_{ElPV.Batt_\tau}^*$: PV power generation stored by the ELSA storage in time step τ as the outcome of the second optimization stage
- $P_{ElBatt.PV.EEG_\tau}^*$: ELSA storage discharging power sold to the EEG in time step τ as the outcome of the second optimization stage
- $P_{ElBatt.PV.District_\tau}^*$: ELSA storage discharging power consumed by the district in time step τ as the outcome of the second optimization stage
- $P_{ElMarket.Batt_\tau}^*$: Power stored by the ELSA storage and traded on the energy trade market by the district operator in time step τ as the outcome of the second optimization stage
- $P_{ElGrid.Batt_\tau}^*$: Power bought from the district's local energy supplier and stored by the ELSA storage in time step τ as the outcome of the second optimization stage.
- $P_{ElBatt.PV.District_\tau}^*$: ELSA storage discharging power consumed by the district in time step τ , which was bought from the district's local energy supplier during earlier time steps as the outcome of the second optimization stage.
- $T_{Batt.PV.Charge_\tau}^*$: Binary decision variable, if the ELSA storage should charge PV power in time step τ as the outcome of the second optimization stage.
- $T_{Batt.PV.Discharge_\tau}^*$: Binary decision variable, if the ELSA storage should discharge PV power in time step τ as the outcome of the second optimization stage.

-
- $T_{Batt.Grid.Charge_\tau}^*$: Binary decision variable, if the ELSA storage should charge power from the district's local energy supplier in time step τ as the outcome of the second optimization stage.
 - $T_{Batt.Grid.Discharge_\tau}^*$: Binary decision variable, if the ELSA storage should discharge power from the district's local energy supplier in time step τ as the outcome of the second optimization stage.